CONVERSION OF CARBON DIOXIDE TO METHANOL OVER VISIBLE LIGHT RESPONSIVE CATALYST

MARIOTTE ANAK PATRICK JEBI

Thesis submitted in partial fulfilment of the requirements
for the award of the degree of
Bachelor of Chemical Engineering

Faculty of Chemical & Natural Resources Engineering
UNIVERSITI MALAYSIA PAHANG

JUNE 2017

UNIVERSITI MALAYSIA PAHANG

DECLARATION OF THESIS AND COPY RIGHT

Author's Full Name : _____MARIOTTE ANAK PATRICK JEBI_____

Date of Birth : _____30/08/1993_____

Title _____

_____

Academic Session : _____

I declared that this thesis is classified as:

☐ **CONFIDENTIAL** (Contains confidential information under the Official Secret Act 1972)*

☐ **RESTRICTED** (Contains restriction information as specified by the organization where research was done)*

■ **OPEN ACCESS** I agree that my thesis to be published as online open access (Full text)

I acknowledge that University Malaysia Pahang reserve the right as follows:

1. The Thesis is the Property of University Malaysia Pahang.

2. The Library of University Malaysia Pahang has right to make copies for the purpose of research only.

3. The Library has the right to make copies of the thesis for academic exchange.

Certified By:

_____   _____
(Student's Signature)   (Supervisor's Signature)

_____   _____
New IC /Passport Number   Name of Supervisor
Date: Date:

NOTES : *If the thesis is CONFIDENTIAL or RESTRICTICTED, please attach with the letter from the organization with period and reasons for confidentiality or restriction

SUPERVISOR'S DECLARATION

We hereby declare that we have checked this thesis and in our opinion, this thesis is adequate in terms of scope and quality for the award of the degree of Bachelor of Chemical Engineering.

Signature   :

Name of main supervisor   :

Position   :

Date   : 20 JUNE 2016

STUDENT'S DECLARATION

I hereby declare that the work in this thesis is my own except for quotations and summaries which have been duly acknowledged. The thesis has not been accepted for any degree and is not concurrently submitted for award of other degree

Signature   :
Name   : MARIOTTE PATRICK JEBI
ID Number   : KA13162
Date   : 20 JUNE 2016

Dedicated to my family and friends

ACKNOWLEDGEMENT

ABSTRACT

The significant increase of carbon dioxide contributed for the largest share of the world's greenhouse gas emissions. There is a growing need to mitigate CO_2 emissions. One of the strategies to mitigate CO_2 emissions is using CO_2 as a raw material in chemical processes. In the present study, a TiO_2 loaded copper (II) oxide (CuO) photoelectrode was synthesized, characterized and studied for photoelectrocatalytic (PEC) reduction of carbon dioxide (CO_2) into methanol under visible light ($\lambda > 470$ nm) irradiation. In this perspective, The material was constructed via sol-gel method from copper (II) nitrate, $Cu(NO_3)_2.3H_2O$ (99 %) and commercial Degussa P25 TiO_2 as precursors. The photocatalysts were characterized by X-ray diffraction, UV-vis absorption specra, X-ray photoelectron spectroscopy (XPS), photoluminescence spectrophotometer, and mott schottky (MS). Linear sweep voltammetry (LSV) was employed to evaluate the effect of visible light ($\lambda > 400$ nm) on the CO_2 reduction reactions. The characterization results indicated that the band gap energy of the $CuO-TiO_2$ catalyst from UV-Vis is 1.39 eV. The flat band potential calculated from the MS data as 0.83 V versus normal hydrogen electrode (NHE). The LSV the dark and under visible light irradiation further support the visible light-responsive photocatalytic activities $CuO-TiO_2$ giving onset potential value from -0.20 V with current peak potential appearing at -0.35V (vs NHE) suggesting an increase in photocurrent and occurrence CO_2 photoreduction reaction. The PEC performance of $CuO-TiO_2$ photocatalyst showed an increased methanol yield of 20.1 $\mu mol.L^{-1}.cm^{-2}$ under visible light irradiation.

ABSTRAK

Peningkatan besar karbon dioksida menyumbang sebahagian terbesar pelepasan gas rumah hijau di dunia. Pelbagai kajian telah dijalankan untuk mengurangkan pelepasan CO_2. Salah satu strategi untuk mengurangkan pelepasan CO_2 adalah menggunakan CO_2 sebagai bahan mentah dalam proses kimia. Dalam kajian ini, yang TiO_2 dimuatkan kuprum (II) oksida (CuO) photoelectrode telah disintesis, ciri-ciri dan dikaji untuk photoelectrocatalytic (PEC) pengurangan karbon dioksida (CO_2) ke dalam metanol di bawah cahaya yang boleh dilihat ($\lambda > 470$ nm) penyinaran. Dalam perspektif ini, bahan ini telah dibina melalui kaedah sol-gel dari kuprum (II) nitrat, $Cu(NO_3)_2.3H_2O$ (99%) dan komersil Degussa P25 TiO_2 sebagai pendahulu. The photocatalysts telah disifatkan oleh X-ray pembelauan, UV-vis penyerapan specra, X-ray spektroskopi fotoelektron (XPS), photoluminescence spektrofotometer dan mott Schottky (MS). Linear voltammetri (LSV) telah digunakan untuk menilai kesan cahaya yang boleh dilihat ($\lambda > 400$ nm) mengenai reaksi pengurangan CO_2. Keputusan pencirian menunjukkan bahawa tenaga jurang jalur daripada pemangkin CuO-TiO_2 dari UV-Vis 1.39 eV. Potensi band rata dikira dari data MS sebagai 0.83 V berbanding elektrod hidrogen biasa (Nhe). The LSV gelap dan di bawah sinaran cahaya yang boleh dilihat terus menyokong kelihatan aktiviti photocatalytic cahaya responsif CuO-TiO_2 memberi nilai potensi bermulanya dari -0.20 V mempunyai potensi puncak semasa yang terdapat di -0.35V (vs NHE) mencadangkan peningkatan dalam arusfoto dan kejadian CO_2 reaksi photoreduction. Prestasi PEC daripada CuO-TiO_2 fotokatalis menunjukkan hasil metanol meningkat 20.1 $\mu mol.L^{-1}.cm^{-2}$ di bawah sinaran cahaya yang boleh dilihat.

TABLE OF CONTENTS

LIST OF TABLES

LIST OF FIGURES

LIST OF SYMBOLS

$^\circ$	Degree
$^\circ C$	degree celcius
Psi	pascal
$e\text{-}$	Negative electron
eV	electron volt
g	gram
ΔG°	standard Gibbs energy change
λ	lambda wavelength
h	hour
kJ/kg	kilojoules per kilogram
$h+$	positive electron
M	molarity
mA	mili ampere
mL	mili litre
nm	nanometer

LIST OF ABBREVIATIONS

CCS   Carbon Capture & Sequestration

CuO   Copper Oxide

CO_2 Carbon dioxide

CH_3OH Methanol

EC   Electrochemical

MS   Mott Schottky

NHE   Normal hydrogen Electrode

TiO_2 Titanium dioxide

PC   Photocatalytic

PEC   Photoelectrochemical

UV   Ultra violet

UV-Vis   UV-Visible

XRD   X-Ray diffraction

XPS   X-Ray Photospectroscopy

CHAPTER 1

INTRODUCTION

1.1   Background of the Study

Fossil fuels such as coal, natural gas and oil is a non-renewable resources of energy from the plant and organic materials decomposition which took millions of year to form. Nowadays, the development of our modern lifestyle demanded continuous energy consumption to provide us with power, heat and fuel supply. Often, by burning of fossil fuels in power plants, has produced a large-scale addition of CO_2 at the atmospheric level which is much faster than the natural processes can remove it. Therefore, multiple concern to find different strategies and technologies to reduce CO_2 emission due environmental issues, greenhouse gas emission.

Carbon capture and sequestration (CCS) technologies is one of the way to reduce CO_2 emission where CO_2 removal and capture from large point sources of industrial processes and are injected and stored in various sinks. However, CCS requires optimisation in order to fill the gap in knowledge with regards to the location, possible geological location capacity and possible leakage during or after injection (Bachu et al., 2007).

Apart from CCS, several methods have been studied to convert CO_2 by using solar energy into a valuable components such as biological reduction by plants and thermal, electrochemical or photocatalytic reduction. The most promising methods, photoreduction CO_2 is therefore are economically cheap, safe and ecologically clean.

In this study, the appropriate photocatalyst are important factors in photoelectrocatalytic reduction of CO_2. Mostly used semiconductor materials, wide bandgap of TiO_2. However, its use is limited due to its large band gap; as it can only be

activated by ultraviolet (UV) light which represents 2–5% of sunlight (Carp et al.,2004). Coupling TiO_2 with transitional metal, CuO shows improvement of the stability in applied photcatalysis. Since copper oxides suffer from photo corrosion and doping with wider band gap of TiO_2, stability will increase therefore contribute to the photoelectrocatalytic efficiency.

The main product from photo catalytic reduction of CO_2 is methanol. Methanol is a colourless, flammable liquid used in the manufacture of formaldehyde and acetic acid Methanol can be prepared from various sources, such as natural gas, coal, biomass and petroleum. The applications of methanol is primarily used as feedstock of other chemical. The advantages of using methanol includes lower production cost compared with other alternative fuels and its safety to lower risk of flammability.

1.2   Motivation

Carbon dioxide is a thermodynamically stable compound formed during combustion of non-renewable fossil fuels and cutting of trees that could intensify net CO_2 emissions and finally posed an environmental threat for the Earth's climate. The accumulation of CO_2 can be prevented by various way such as removal, storage and sequestration. Other than that, research studies several conversion methods including biocatalysis, thermocatalysis, photocatalysis, electrolysis and photoelectrocatalysis (PEC) to obtain a sustainable fuel products, methanol, methane, formic acid and formaldehyde (Ampelli et al., 2016). In addition, high energy density by volume and by weight, able to store at low pressure in room temperature and low toxicity are the benefits of producing methanol from CO_2 (Ganesh, 2014). In order to lower CO_2 level, an alternative approach is through photocatalysis as it is advantageous by lowering of the recombination rate of photogenerated electron holes, thus produce higher efficiency.(Nikokavoura & Trapalis, 2016). The photocatalytic reduction of CO_2 requires multiple electron transfers and can lead to the formation of many different products depending on the specific reaction pathway taken. Nevertheless, introducing defects in photocatalyst could improve electron-hole separation and act as sink onto phototcatalyst surface, enhance the separation of electron–hole pairs and to improve the photocatalytic efficiency. .

In this study, CuO loading on TiO_2 to further explain their performance on methanol yield at the same time tries to bring some light into relationship between physico-chemical properties of TiO_2 doped by CuO for photoelectrochemical reduction efficiency. Koči et al., 2014 reported that coupling of two oxide semiconductors provides a novel approach to promote a charge separation, increase a lifetime of the charge supports and enhance an interfacial charge transfer to adsorb substrate. In order to improve the solar conversion efficiency, great efforts have been made to extend the useful response of TiO_2-based material to the visible region. CuO loaded TiO_2 catalyst showed promising performance as visible light active catalyst for CO_2 reduction. CuO could act as electron tank reducing the e^-/h^+ recombination rate. Further incorporation of metal oxide metal nanoparticle can create the schottky barrier and improving the

photoelectrochemical performance. To the best of our knowledge, CuO-TiO_2 photocatalyst has never been investigate for CO_2 reduction under visible light.

1.3 Problem Statement

The increasing of CO_2 nowadays are at its alarming level in environment since the beginning of industrial age, such as deforestation and fossil fuels consumption raising serious environmental issues, greenhouse effect. To overcome this difficulty, many researchers actively to develop photocatalysts in effort to enhance the efficiency of CO_2 reduction into a value added chemical, methanol under visible light and illumination of solar. However, the capture and reduction of rather inert and stable CO_2 compound requires high energy temperature and pressure input (Sarkar et al., 2016). Photocatalysis (PC) as it is advantageous multiple electron transfers and can lead to the formation of many different products depending on the specific reaction pathway taken but typically suffers from slow kinetics, poor product selectivity and mechanistic complexity (Tu, et al., 2014). Apart from that, semiconductor TiO_2 is the most studied photocatalysts with wide band gap of 3.2 eV limits its optical absorption only within ultraviolet light region, <387 nm and minimises it solar energy conversion efficiency (Wang et al., 2016). One fundamental weakness that has limited the use of photochemical reactions on industrial scales is the inability of most organic molecules to absorb visible wavelengths of light. Thus it is desirable to synthesize a photocatalyst and examine its chemical efficiency for conversion of carbon dioxide to methanol under the visible light via photoelectrochemical reduction.

1.4   Objectives

The main objective of this research is to synthesize and characterize CuO-TiO_2 as a light responsive catalyst that used in CO_2 photoelectrochemical reduction into methanol under visible light irradiation.

1.5   Scopes of Study

The following are the scope of this research:

1)   The copper nanoparticles on TiO_2 was prepared in the molar ratio of 1:1 by sol-gel method.

2)   The CuO-TiO_2 as a photocatalyst for the photoelectrocatalysis of CO_2 reduction to methanol over visible light radiation.

3)   Characterisation of the synthesised catalyst was investigated through Ultraviolet-visible (UV-VIS) absorption spectroscopy, X-ray diffraction (XRD), and X-ray photoelectron spectroscopy (XPS) analysis, Photoluminescence and Mott Schottky.

4)   The formation of methanol was qualified by GC-MS and quantified by Gas Chromatograph Flame Ionization Detector (GC-FID).

CHAPTER 2

LITERATURE REVIEW

2.1 Introduction

The increment in the utilization of fossil fuels has resulted a significant increase in environmental CO_2 from preindustrial levels of 280 ppm to daily mean environmental concentration of CO_2 was at 400.06 ppm was seen at Syowa Station, Antarctica, on May 14, 2016 in Figure 2.1 (Watt, 2016). A worldwide temperature alteration is fundamentally an issue of an excess of carbon dioxide in the environment. This excessive carbon is caused mainly when we burn fossil fuels like coal, oil and gas or cut down and burn forests. There are many heat trapping gasses from methane to water vapor, yet CO_2 are the most serious danger of irreversible changes that it keeps on aggregating tireless in the climate.
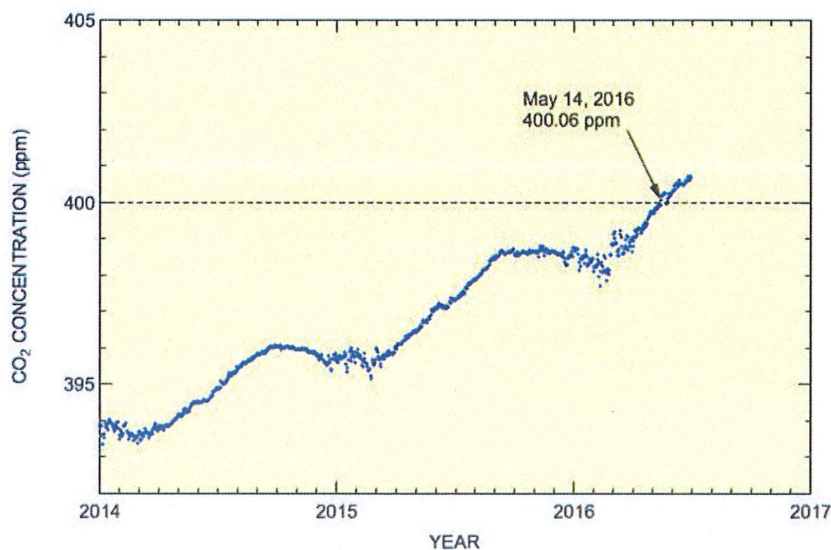
Figure 2-1: CO_2 concentration observed at Syowa Station since 2014 (Watt, 2016).

The physical properties of CO_2 are described as a slightly odour and colourless and heavier than air. It can freezes at -78.5 °C to form CO_2 snow and the density is 1032 kg/m^3. In addition, for chemical properties of CO_2, it has vapour pressure about 58.5 bar and latent heat of vaporization at 571.08 kJ/kg. Although CO_2 is nontoxic and bacteriostatic, but it still can harm to the environment that cause greenhouse effect. Therefore, study has been made to lessen the amount of CO_2 at the atmosphere by photcatalysis method. An artificial photosynthesis or commonly known as photocatalysis is a process to speed up of photoreaction by using light responsive catalyst in CO_2 reduction. The idea of synthetic photosynthesis comes from the process of natural green plants photosynthesis that also converts CO_2 and H_2O into organic product as well as CO.

2.2   Thermodynamic considerations of CO_2 reaction

CO_2 photoreduction is a multiple-step reaction. During transfer of one electron, the structure changes from linear to bent form. However, an extensive input of energy, optimized reaction conditions along with very active catalyst are needed for any chemical conversion of CO_2 to fuel. Despite that, chemical reactions are motivated only by difference in Gibbs free energy between reactants and products of the reaction process.

Since a quite inert and stable linear molecule of CO_2 ($\Delta G° = -400$ KJ mol^{-1}) consist of a carbon atom that is having two double bonds and two oxygen atoms, $O = C = O$, this has made the reduction of CO_2 quite challenging without help of any catalyst and input energy. Karamian & Sharifnia (2016), stated that adsorption of CO_2 onto a photocatalyst surface is the best way for lowering its energy barrier, because the structure of CO_2 transforms to a bends form and thus it shows a high reactivity.

Although reduction of CO_2 to hydrocarbon fuel or fuel precursor by photocatalytic is blatantly obvious in principle, but thermodynamic view point is not too favourable because they usually suffer from slow kinetics, poor product selectivity and mechanistic complexity (Tu, et al., 2014). As can be seen from table 2.1, with the 6 electron reduction of CO_2 to methanol by proton having standard potential of only -0.38V based in pH 7 in aqueous solution versus NHE, 25°C, 1 atmosphere gas pressure, and 1 M for the other

solutes. In contrast, the single electron reduction of CO_2 to $\bullet CO_2^-$ occurs at -1.90 V, equation 2.1, due to a large reorganizational energy between the linear molecule and bent radical anion (Benson, Kubiak, Sathrum, & Smieja, 2009).

Table 2.1 Carbon dioxide reduction standard potentials at pH 7.0 versus NHE

Reaction Pathway	$E°/V$ (vs. NHE)	
$CO_2 + 2H^+ + 2e^- \rightarrow CO + H_2O$	-0.53 V	(2.1)
$CO_2 + 2H^+ + 2e^- \rightarrow HCOOH$	-0.61 V	(2.2)
$CO_2 + 4H^+ + 4e^- \rightarrow HCHO + H_2O$	-0.48 V	(2.3)
$CO_2 + 6H^+ + 6e^- \rightarrow CH_3OH + H_2O$	-0.38 V	(2.4)
$CO_2 + 8H^+ + 8e^- \rightarrow CH_4 + 2H_2O$	-0.24 V	(2.5)
$CO_2 + e^- \rightarrow {}^\bullet CO_2^-$	-1.90 V	(2.6)

2.3 Visible light photocatalytic activity

Light can be considered an ideal reagent for environmentally friendly, greener chemical synthesis whereas unlike many conventional reagents, light is non-toxic, generates no waste, and can be obtained from renewable sources. Most of the organic molecules photochemical reactions on industrial scales unable to absorb visible wavelengths of light. Nevertheless, the ultraviolet wavelengths generally required in conventional organic photochemical synthesis are not abundant in the solar spectrum. As a consequence, the practicality and environmental benefits of photochemical synthesis on industrially relevant scales has its own limitation (Yoon, Ischay, & Du, 2010).

The design of a photocatalyst for the utilization of solar energy as a motive power is considered one of the most promising and clean approaches towards pollutant removal from the environment. Based on Yihong Qiu et. al (2009), ultraviolet (λ=200-400nm), visible light (λ=400-800nm) and infrared (λ>800nm). The ultraviolet energy can specifically activate the chemical bonds of a few organic molecules to give exceedingly responsive radical intermediates, which brings about poor selectivity of the product. In

addition, the infrared wavelength with similarly low vitality can't meet the prerequisite of actuation vitality for by far most of natural responses.

Visible light is abundant in nature compared to the ultraviolet and infrared where through visible light, reflection & refraction are easily observed. However, it generally could not be adsorbed directly by reactant molecules to drive the reaction. Therefore, visible light photocatalyst employed as a bridging media for the energy transfer between visible light and substrates will be of particular importance. TiO_2 is a UV light driven photo catalyst but researcher have tune its band gap to make it active for visible light photoelectrocatalysis.

2.4   General principle of CO_2 reduction reaction

2.4.1   Photocatalysis (PC) reaction

The word "photocatalysis" has a Greek origin and comprises of two parts: the prefix Photo (phos: light) and the word catalysis (katalyo: break apart, décompose). Photocatalytic reduction of CO_2 has become an interesting research topic because of the potential utilization of renewable solar energy. Figure hotocatalysis is a process in which the absorption of light photons having energy equal to or greater than the band gap energy

Typical mechanisms of CO_2 photoreduction occurs as shown in Figure 2-2, when an electron excited by light energy, its transferred from the fully occupied holes in valence band (VB) to the bottom of the empty conduction band (CB) leading to an equal number of vacant holes. Next, migration of the resultant electrons and holes took placed from inside of the semiconductor until they reach the surface. Reaction occurs between electron and holes with CO_2 (HCO_3^-, CO_3^{2-}) and H_2O that adsorbed on the surface. Therefore, reduction of CO_2 by photogenerated electron can form hydrocarbon CH_4, whereas O_2 generation from the oxidation of H_2O by the holes (Guo et al.,2016)
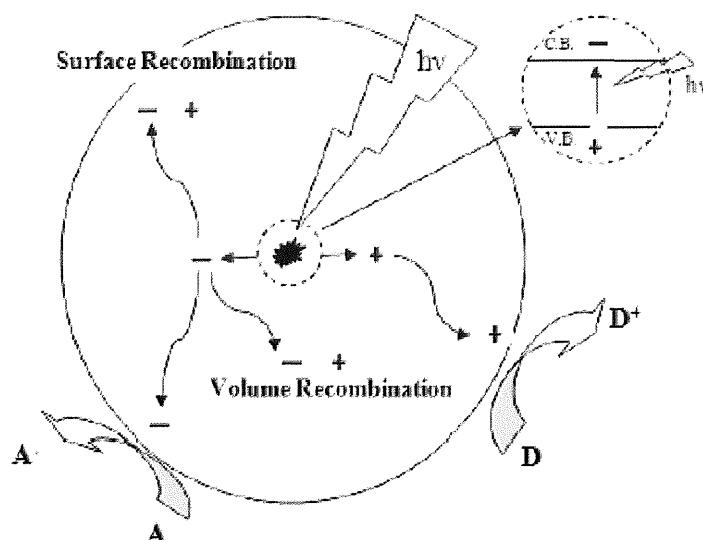
Figure 2-2: Schematic of band gap formation and photocatalytic reaction where CB and VB is conduction band and valence band respectively (Ola & Maroto-valer, 2015).

Besides that, the main products derived from a photocatalytic conversion of CO_2 are strongly dependent on the type of photocatalyst used. The control of product selectivity requires further understanding on the rate determining step leading to the formation of each product. Therefore, electrochemical CO_2 reduction is one of the method to control of product selectivity by applying overpotential to achieve the desire product.

2.4.2   Electrochemical (EC) reduction

The electrochemical reduction of CO_2 usually requires a high potential of nearly 2 V vs. NHE for a one electron process. By performing a two electron or proton coupled multi-electron CO_2 reduction, however, the required potential can be lowered significantly (Portenkirchner et al., 2012). An electrocatalyst both participates in an electron transfer reaction (at an electrode) and facilitates acceleration of a chemical reaction. A main challenge in electrochemical CO_2 reduction is to develop catalysts that are capable of reducing CO_2 beyond the two-electron products carbon monoxide (CO), formic acid (HCOOH), and oxalate ($C_2O_4^{2-}$). Unfortunately, the formation of reduction products requiring four or more electrons is regularly associated with considerable

10

subjected to overpotentials due to the multiple intermediates involved in the reaction mechanisms which eventually reduce the conversion efficiency. In the general sense, electrocatalysts are electron transfer agents that ideally operate near the thermodynamic potential of the reaction to be driven, E^0(products/substrates). A general approach for an electrocatalytic system is given in Figure 2.3.
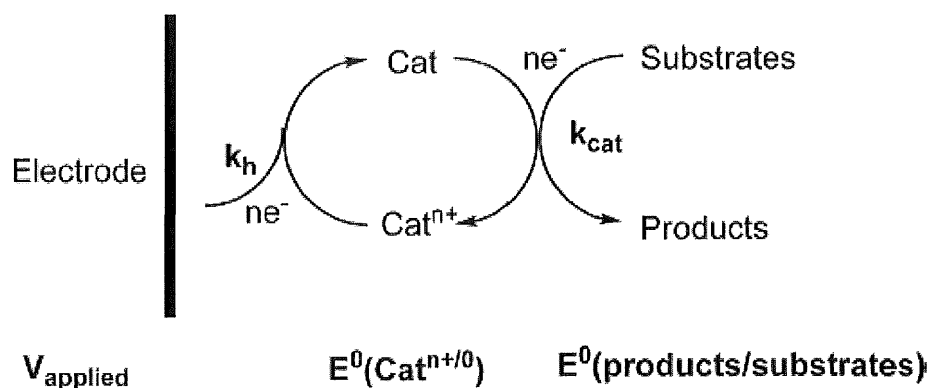
Figure 2-3: Schematic of electrocatalysis with electron source (Benson et al., 2009).

Direct electrochemical reduction of carbon dioxide on most electrode surfaces requires large overvoltages which consequently lowers the conversion efficiency. The overvoltage can be considered to be the difference between the applied electrode potential, $V_{applied}$, and E^0 (products/substrates), at a given current density. Both thermodynamic and kinetic considerations are important here. Clearly, in order to minimize overvoltages, catalysts need to be developed that have formal potentials, E^0 ($Cat^{n+/0}$) well matched to E^0(products/substrates), and appreciable rate constants, k_{cat}, for the chemical reduction of substrates to products at this potential (Benson et al., 2009). In addition, the heterogeneous rate constant, k_h, for reduction of the electrocatalyst at the electrode must be high for $V_{applied}$ near E^0($Cat^{n+/0}$).

11

Further explanation for the overall reaction of CH_3OH formation is a combination of a reduction and oxidation reaction at the cathode and anode of the system. According to in Albo et. al., 2015, the electrochemical reduction of CO_2. Two reactions took places when the electrical energy is supplied to the system:

(i) Hydrogen Evolution Reaction (HER), in which the energy is consumed for the production of hydrogen through the process of water electrolysis.

(ii) The reduction of CO_2 into the product mainly CH_3OH.

In order to achieve high selectivities for a given product and high yield of the desired CH_3OH, it is required to use an electrode material able to suppress the HER so that most of the electric energy supplied is consumed only in the CO_2 reduction reaction. The employment of aqueous electrolytes in the electrochemical reduction of CO_2. Commonly, alkali cations such as Na^+ and K^+ and various anions such as halide anions (e.g. Cl^-), bicarbonate (HCO_3^-) or hydroxide (OH-) in aqueous solutions. This is because these inorganic salts are often used due to their high conductivities in water and because they can provide the required protons involved in the reaction pathway.

2.4.3   Photoelectrochemical (PEC) reaction

Photoelectrocatalysis is an alternative process that integrates photocatalysis and electrocatalysis which could further enhance the reduction process of CO_2. Photoelectrocatalysis is similar to electrocatalysis in regard to the experimental setup. PEC cell consisted separated half cells of anode and cathode with immobilized photocatalysts electrode connected to a counter electrode and reference electrode on the other cell can avoid re-oxidation of product formation such as methanol (Xie, Zhang, Liu, & Wang, 2015). However, photoelectrocatalysis integrates photocatalysis with electrocatalysis and typically exploits semiconductor electrodes instead of normal conducting electrodes used in electrocatalysis. Photoelectrocatalytic reduction of CO_2 would reduce electricity consumption as compared to the electrocatalytic reduction of CO_2 because of the introduction of solar energy. On the other hand, as compared to photocatalysis, photoelectrocatalysis may achieve higher efficiency because the applied

external bias voltage can help the separation of photogenerated electrons and holes, which is the most crucial step in limiting the photocatalytic efficiency.

Figure 2.4 depicts the schematic illustration of Fujishima–Honda photoelectrochemical (PEC) water splitting cell. A conventional PEC cell consists of two indispensable parts (a) light driven photocatalytic materials assembled on current collectors which are mostly used transparent conducting oxide (TCO) substrates as working electrodes (anode compartment), and (b) metal electrocatalyst (platinum) as counter electrode (cathode compartment). In between the anode and cathode compartments aqueous electrolyte is filled and separate by a proton conducting membrane. Upon photo irradiation, charge carriers are photogenerated at the semiconductor material, and subsequently the photoexcited electrons are injected from the conduction band of semiconductor to charge collector terminal.
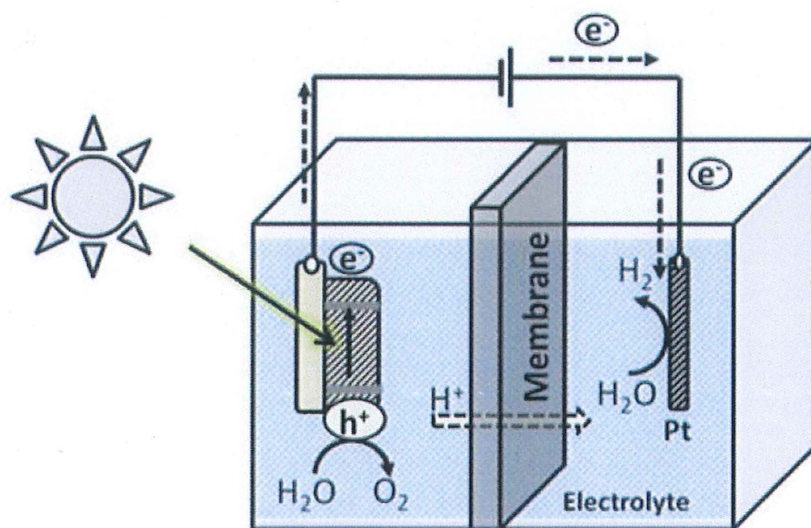
Figure 2-4: Schematic illustration of solar light driven water splitting cells (Sudhagar, Roy, Vedarajan, & Devadoss, 2016)

The first use of a photocatalyst, as a photocathode, for the PEC reduction of CO_2 was reported over 30 years ago. Most of the research on the PEC reduction of CO_2 involves electrically assisted photocatalysis. A small bias is added to the catalyst materials based on PC reduction to effectively separate the photo-generated holes and electrons and achieve higher photoelectric conversion efficiency. However, the applied bias is too small to independently conduct EC reduction. Previously, we reported photo-enhanced

electrocatalysis with efficient reduction efficiency. However, the light itself could not provide the desired PC function independently. Therefore, we combined EC and PC functions to achieve a synergistic function between them on the same catalytic surface (P. Li et al., 2014). To achieve a synergistic function between PC and EC, the selection of a catalyst is key, which requires that the catalyst not only matches the energy band for PC reduction, but also simultaneously matches the small overpotential for EC reduction.

Recently, Brito, et al., 2014 described the photoeletrocatalytic reduction of CO_2 dissolved in 0.1 M Na_2CO_3/$NaHCO_3$ at Cu/Cu_2O electrodes prepared by electrochemical deposition of a Cu foil. CH_3OH yield as high as 80 ppm and a Faradaic efficiency of 75% under UV-Vis irradiation and bias potential of + 0.16 V vs SCE showing the obtained values were very promising. Therefore, the study of photocatalyst performance on CuO-TiO_2 as a visible light responsive catalyst as to increase the photoefficiency of the PEC and product yield.

2.5   Selection of CuO-TiO_2 as photocatalyst

Among the metal oxides available, TiO_2 is a more popular photocatalyst owing to its exceptional properties, such as low cost, high stability, high chemical inertness, biocompatibility, non-toxicity in photocatalytic reduction (Ansari et. al., 2015). TiO_2 can affect the efficiency and selectivity of the methanol produced. The most crucial problem is a low quantum yield in the photocatalysis process due to electron and positive hole recombination. In order to increases yield, TiO_2 must be modified by using dopants of metal. In CO_2 photo-reduction, Yamashita, et al., (2002), reported that the addition of copper could improve the efficiency and selectivity to produce methanol.

While a few reviews have been accounted for to change TiO_2 with noble metals, transition metal oxides and non-metal ions in particular, it has been shown that transition metal oxides such as copper oxide have the potential of enhancing the photoelectrochemical activity of TiO_2. It has been demonstrated that transition metal oxides, for example, copper oxide have the capability of enhancing the photoelectrochemical action of TiO_2.

The dependence of the semiconductor conductance band and redox potential of adsorbate can affect the effectiveness of semiconductor to transfer photo-induced electron toward adsorbed species. Larger band gap of semiconductor shows that the reduction of CO_2 can be made as they can provide enough redox potential to carry out in the chemical reaction. Table 2.1 shows the varieties of band edge positions of photocatalysts for CO_2 reduction.

Table 2.2: Varies of semiconductor of photocatalyst with their band gap energy (Marszewski, Cao, Yu, & Jaroniec, 2015)

Photocatalyst	Band gap energy [eV]
Si	1.1
Cu_2O	1.91
CuO	1.35
CdS	2.4
WO_3	2.8
TiO_2 rutile	3.02
Fe_2O_3	3.1
TiO_2 anatase	3.2

By far, the most common strategy for band engineering is doping with either metal or non-metal heteroatoms; and titania is the most extensively studied in this regard. Photoelectrochemical activity is affected by the properties of a photocatalyst, as well as the reaction condition such as pH, concentration, illumination power and surface area of the crystal (Djurišić et al., 2014). The design of molecular size and modification of catalyst structure has been extensively studied to improve the efficiency. Clearly, various experimental conditions will impact the overall product yield independently of the material's properties.

Inoue et al. (as cited in Li et al., 2016, p. 421) reported the photocatalytic reduction of CO_2 to form organic compounds in the presence of semiconductor. The stability, cheaper TiO_2 and its CB is suitable to trap the high energy electrons and then reduce protons thermodynamically. However, in a real application TiO_2 is not so practical

because its energy band is quite wide, so it can be activated only under the ultraviolet light irradiation.

The efficiency and selectivity of methanol can be affected by TiO_2. In order to increase the methanol yield, TiO_2 can be modified by using metal dopants. Metals doping such as Cu, Pt, and Fe in the TiO_2 can increase the conversion rates. This can be by doping into TiO_2 lattice or by coating the metal oxide on the surfaces of TiO_2. W. N. Wang et al. (2014) stated that at the conduction band of TiO_2, as the injected excited electron travel across the TiO_2 crystal lattice and becomes trapped. This is due to the lower energy state obtained. Thus, decreasing the rate of electron-hole recombination.

Many studies have demonstrated that the addition of Cu cocatalyst to TiO_2 by changing the dynamic structure of electron-hole recombination and interfacial charge transfer and reported yield to be more effective (Tseng et al., 2002). Copper oxides (Cu_xO) can exist in different stoichiometries and phases such as Cu_2O and CuO with narrow band gap energy from 1.2 to 2 e.V. This is due to interesting photochemical and photomagnetic properties of copper oxide among other transitional metals. In most of literature, CuO shape and size-dependent properties are to be consider precisely on the chemical composition, size, shape and surface chemistry to obtain desired chemical and physical properties. Moreover, these copper oxides are all visible-light-active and with the TiO_2 doped CuO, they are expected to be resistant to the photocorrosion of the narrow-bandgap copper oxide making them more useful in the fields of photosynthesis and pollutant treatment.
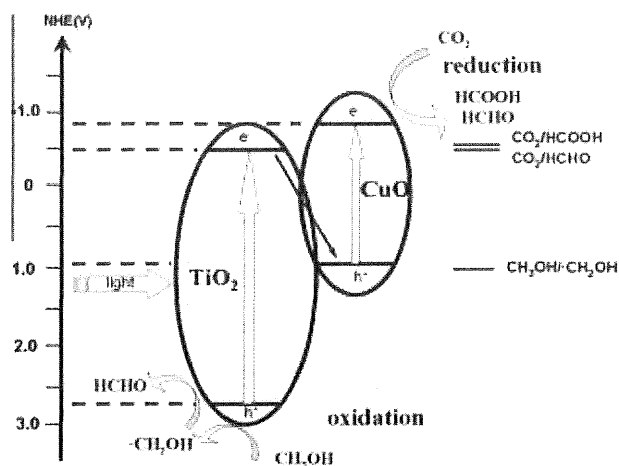
Figure 2-5: Schematic diagram showing the energy band positions of TiO_2, CuO and the electron transfer direction (Qin, Xin, Liu, Yin, & Ma, 2011).

2.5.1 Influence of CuO on TiO_2 Photocatalytic Reduction

Copper can serves as electron trapper and prohibits electron and holes recombination. It was reported by Nasution, et al., (2009), CuO is the most active dopant comparing to other species. The formation of methanol was found to be much more effective on Cu^{2+} loaded TiO_2 catalyst. In selecting copper oxide as dopant is is based on their potential redox position as well as the potential redox value, which is represents their ability to attract electrons.

From a thermodynamic perspective, trapping electron by metal ions (Cu or Cu) within the semiconductor photocatalyst is feasible due to the reduction potential of the metal ions is more positive than the conduction band edge of TiO_2 (-0.2 V). Other than that, the positive potential redox value of Cu is higher than that of Cu^{2+} 0.52 vs. 0.34 V); therefore Cu_2O dopant should effectively act as an electron trapper to prohibit electron-hole recombination. However, since TiO_2 is relatively strong interaction with the dopant particle implanted in the vacant sites of TiO_2, the dopant with more positive potential redox exceedingly catches electron from conduction. Therefore, more difficult to transform the dopant-trapped electrons into the adsorb species on the catalyst surface.

17

Comparing to that, Cu^{2+} with the lower potential redox is a more promising dopant species. Due to the reduction of Cu^{2+} is thermodynamically feasible and a Cu^{2+} ion has an unfilled 3d shell, it is valid to assume that electrons can be trapped by $Cu^{II}O$ on the surface of TiO_2. Further explaination can be illustrated in figure 2.6 and equation 2.7 of the redox cycle of Cu^{2+}/Cu^+ that maybe played by CuO dopant on the TiO_2 matrix. It can be explain that, part of the photo-excited electrons on the conduction band (e_{CB}^-) will be trapped by Cu^{2+}, consequently the species of Cu^{2+} can be reduced to Cu^+ species. Then, trapped electron could be consumed via the reduction of H^+ and/or O_2 that present in the system forming radicals of $\bullet H$ and/or $\bullet O_2^-$ respectively. Finally, the Cu^+ species could be re-oxidized again to Cu^{2+} species (Kakumoto,1995). This cycle of process resulting the reduction of the electron-hole recombination rate.

$$Cu^{II}O \rightarrow Cu^{I}O \rightarrow Cu^{II}O \tag{2.7}$$
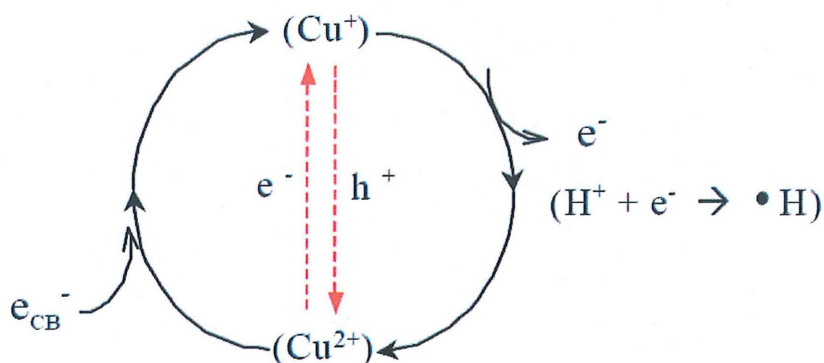
Figure 2-6: Schematic of the redox cycle of Cu^{2+}/Cu^+ system in the photoreduction of CO_2 (Nasution et al., 2009)

CHAPTER 3

METHODOLOGY

3.1   Chemical

Copper (II) nitrate trihydrate ($Cu(NO_3)_2.3H_2O$), Titanium (IV) Oxide (TiO_2), are all 99% is of analytical grade, absolute technical grade 99%, hydrazine monohydrate ($N_2H_4. H_2O$) and sodium bicarbonate ($NaHCO_3$) from Merck were used as received. No further purification was required.

3.2   Preparation of CuO-TiO$_2$

The synthesis of CuO-TiO$_2$ nanoparticles were prepared briefly as follows. A required amount of $Cu(NO_3)_2.3H_2O$ amd TiO_2 Degussa-P25 powder, and ascorbic acid (0.02M) were was dispersed into the solution of 50 ml distilled water. 11 mL reducing agent $N_2H_4 \cdot H_2O$ (0.347 M) was pipetted into the reaction mixture with continuous stirring at room temperature for ~ 4 h until colour changes from blue to red precipitate (Ramli et al., 2014). After that, the mixture was transferred to sonicator bath for further reaction at 70°C until form a thick paste. The paste sample are kept in vacuum oven at 70°C, 0.5 MPa for overnight drying. Finally, the sample was crushed into a fine powder using marble mortar and was kept in the vial for analysis. The same procedure were repeated to give copper content between 0.75:0.25 CuO-TiO$_2$ and 0.25:0.75 CuO-TiO$_2$.

$$Cu^{2+} + N_2H_4 + 4OH^- \rightarrow Cu + N_2 + 4H_2O \qquad (3.1)$$
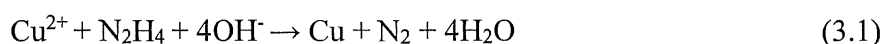
The electrode preparation were described by (Khan et al. 2015); Woon et al. (2015). Catalyst ink was prepared by mixing 22 mg of CuO-TiO$_2$ with 140 μL of 5 wt% Nafion and 280 μL isopropanol (C_3H_8O) and was transferred to sonicator bath for 30 min.

Thereafter, the ink was evenly brushed with an area of 1 cm^2 of graphite paper as illustrated in figure 3.1. The electrode was dried in vacuum oven at 70 °C for 6 h.
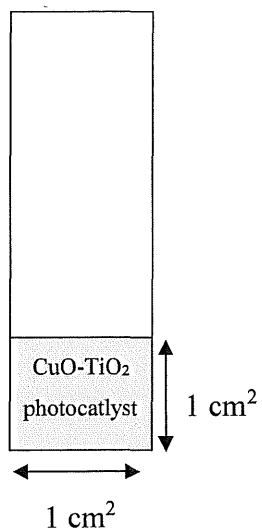
Figure 3-1: 1 cm^2 CuO-TiO$_2$ photocatalyst on graphite paper

3.3   Material Characterization of Photocatalysts

3.3.1   UV–vis diffuse reflectance spectra

Ultraviolet-visible (UV-VIS) absorption spectroscopy and estimation of catalysts bandgap was conducted by Shimadzu UV-2600 where $BaSO_4$ as reference. To calculate valence band position, the optical band gap was determined by the following Tauc equation (Mathai, 2014):

$$(\alpha h v) = B[hv\text{-}E_g]^m \tag{3.1}$$

where B is the absorption coefficient, E_g is the optical band gap energy, h is Planck's constant, v is the frequency of incident photon, and m is an index which depends on the nature of electronic transition responsible for the optical absorption. Values of m for allowed direct and indirect transitions are 1/2 and 2, respectively. Optical transitions of the samples under study are indirect one. The indirect optical energy gap can be obtained from the intercept of the resulting linear region with the energy axis at $(\alpha h v)^{1/2} = 0$.

3.3.2   X-ray diffraction (XRD)

The catalysts were investigated by X-ray diffraction of the powder were obtained at room temperature using Rigaku MiniFlex II at Bragg angle of $2\theta = 10 - 80°$ with a scan step of 0.02°. The The measurements were performed at 30 kV and 15 mA using Cu-Kα emission and a nickel filter. The crystallite size of the prepared nanocomposite was also determined from the XRD spectra and the particle size will be determine from the broadening of the diffraction peak using Scherrer formula (Saito et al., 2015) (Prasad et al. 2016; Uddin et al. 2015). Preparation of 1g samples were compressed in a cylindrical mold with a pressure of 1 MPa on top of the disc specimen of the samples.

$$D = \frac{K\lambda}{BCos\theta} \tag{3.2}$$

Where, D is the coherent scattering length (crystallite size), K is a constant related to crystallite shape whose value is approximately 0.9, λ is the X-ray wave length of $Cu - K\alpha$ radiation source $= 0.154118$ nm and B (in rad) is the full width of half-maximum (FWHM) of the peak, determine by Gaussian fitting.

3.3.3 X-ray Photoelectron Spectroscopy

X-ray photoelectron spectroscopy (XPS) is a quantitative spectroscopic method that determined the elemental-composition, kinetic energy, empirical-formula, chemical-state, binding energy, and electronic-state of the elements that present within a material. XPS spectra are acquired by irradiating a material with a beam of X-rays, while simultaneously determining the kinetic energy and number of electrons that get-away from the top one to ten nm of the material being analyzed. Here, XPS measurements were executed for CuO-TiO2 X-ray photoelectron spectroscopy (XPS) measurement was conducted to determine the chemical states of the sample surface using PHI 5000 versa probe.

3.3.4 Photoluminescence Spetroscopy

Recombination rate of photogenerated electron-hole pair (e^-/h^+) was estimated using Perkin Elmer LS 55 Luminescence spectrophotometer. The luminescence is analyzed with a spectrometer and the peaks in the spectra represent a direct measure of the energy levels in the semiconductor. Photoluminescence (PL) spectra were conducted using a Renishaw 1000 Raman system using a l=325 nm laser at room temperature

3.3.5 Mott Schottky

The following information analysed on the (CuO-TiO$_2$) contact properties from capacitance measurements by considering capacitance-voltage relationship of conducting photocatalyst flat band potential (Vfb) based on equation 3.3.

$$\frac{1}{C^2} = \frac{2}{\varepsilon_0 \varepsilon_r e N_A} \left(V - V_{fb} - \frac{K_B T}{e} \right)$$ (3.3)

Here N_A is the carrier density, ε_0 is the permittivity in vacuum; ε_r is the relative permittivity; V is the applied potential and T is the absolute temperature. Value e is the electronic charge, and k_B is the Boltzmann constant. Hence a plot of $1/C^2$ versus potential (*V*) will yield a line, which when extrapolated to the x-axis, will correspond to the flat-band potential of the semiconductor (Moniz et. al., 2015).

Mott-Schottky analysis was carried out by using an electrochemical analyser (Autolab Compact PGSTAT 204, Netherland) with a $CuFe_2O_4$ electrode, platinum foil, Ag/AgCl electrode and non-CO_2 bubbled 0.1 M $NaHCO_3$ solution (pH 6.8) were used as a working electrode, counter electrode, reference electrode and electrolyte, respectively.

3.4 Photoelectrocatalytic Measurements

Photoelectrocatalytic reduction of CO_2 will be carried out in a Plexiglas quartz window equipped with three-electrode system, CuO-TiO_2 were used as the working electrode, Ag/AgCl reference electrode and a platinum foil as the counter electrode with compartments for water oxidation and CO_2 reduction as illustrated in figure 3.1. Linear sweep voltammetry (LSV) was performed at the applied potential of -0.20 to -1.2 V at a scan rate of 0.05 V.s^{-1}. The amperometric *i-t* curve was recorded at a constant potenial by setting the onset potential obtained from LSV experiment with an interval of 200 s. Other than that, electrochemical impendence spectroscopy (EIS) was performed at the open circuit potential (OCP) using light filter of 470 nm for light off and light on. All of the experimental data was conducted using analogue circuit with the NOVA 1.10 software installation connected with an Autolab PGSTAT302N potentiostat/galvanostat.

Electrolyte solution of 0.1 M sodium bicarbonate, $NaHCO_3$ were used in anodic and cathodic compartment and was bubbled up and carbon dioxide gas through the solution for 30 min at a flow rate of 20 mL.min^{-1} until the concentration of CO_2 reached saturation before illumination started. Blank tests were carried out under light without

CHAPTER 4

RESULTS AND DISCUSSION

4.1 Introduction

Photoelectrocatalytic reduction of CO_2 of as-prepared CuO-TiO_2 through sol-gel method has been carried out on sodium bicarbonate, $NaHCO_3$ solution.

4.2 UV-Vis Spectroscopy Analysis

The UV-vis spectra of as-prepared CuO-TiO_2 (CuO loading to TiO_2 was 1:1 molar ratio) and commercial TiO_2 (calcined at 500°C) in the wavelength range of was measured with a Shimadzu UV-2600 UV-Vis Spectrophotometer. Figure 4.1 (a) depicted depicted the transparency for wavelength above 200 and 1000 nm which shows the visible light activity of the photocatalysts. The UV-vis spectra of as-synthesised CuO-TiO_2 and commercial TiO_2 (calcined at 500°C). Tauc plot which represents the indirect transition of band gap energy values by plotting $(\alpha h\upsilon)^{1/2}$ versus $h\upsilon$ as shown in figure 2(b). The band gap of the commercial TiO_2 are 3.2 eV which correspond to wavelength absorption of 397 nm and CuO-TiO_2 with a higher intensity of absorption displayed lower optical band gap energy of 1.39 eV as expected for CuO according to literature reports (Moniz et al., 2015). Therefore, our as-prepared CuO-TiO_2 had a red shift which enhanced photoabsorption towards the visible light region.
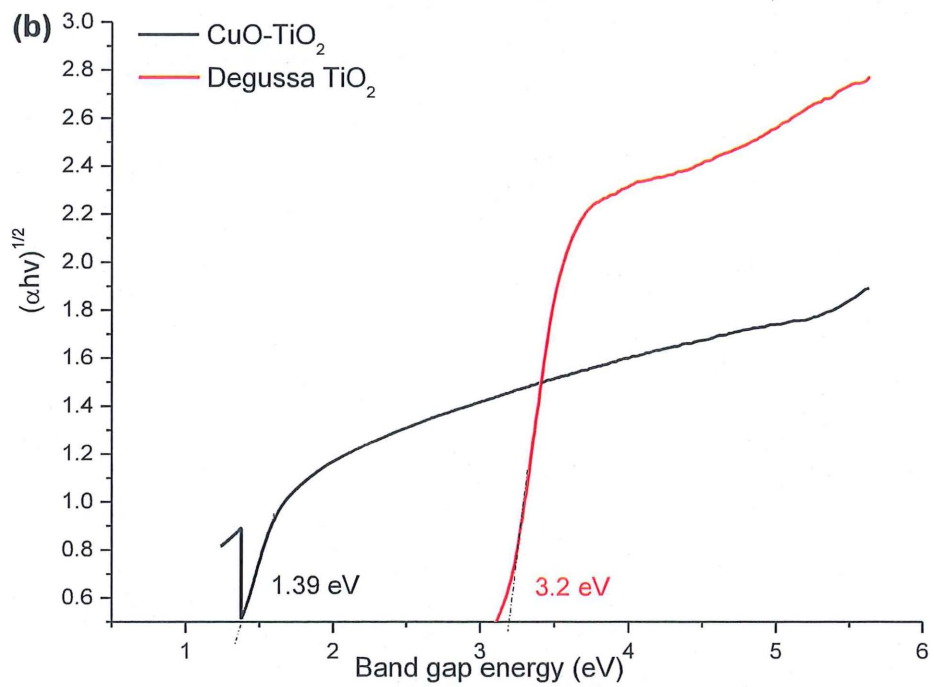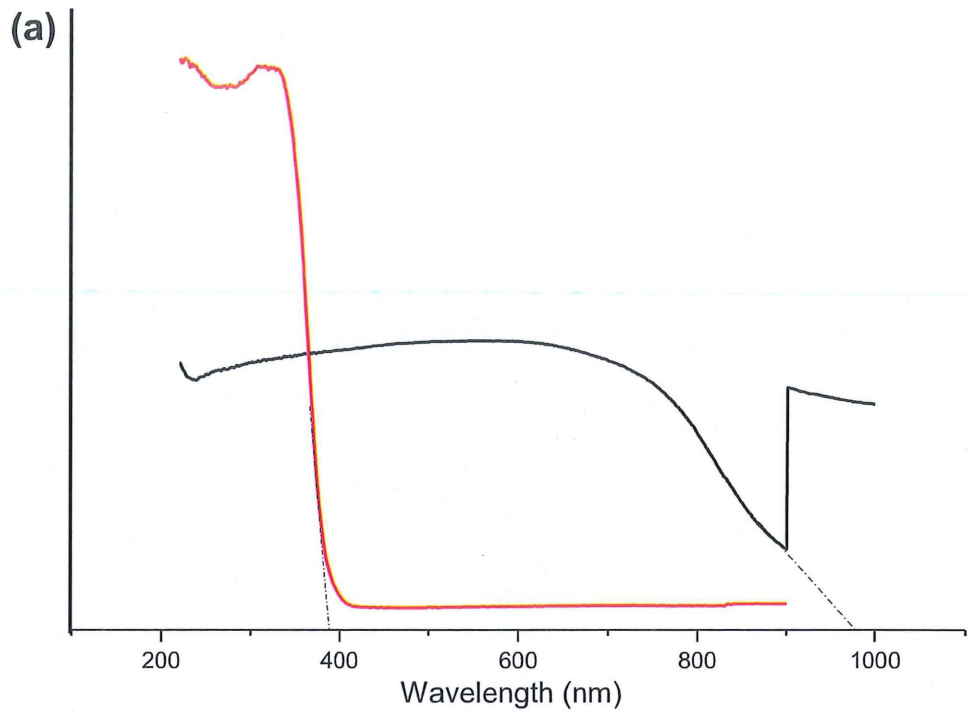
Figure 4-1 (a) UV-Vis spectrum of prepared CuO-TiO₂ photocatalysts. **(b)** Band gap energy calculation of prepared photocatalysts.

4.3 X-ray Diffraction (XRD) Analysis

The XRD diffraction patterns of the CuO-TiO$_2$ are shown in 4.2. The strong and sharp diffraction peaks indicate the high crystalline quality of the samples. It can be seen that all the indexed diffraction peaks in the XRD pattern show the presence of monoclinic CuO in tenorite phase (Barreca et al., 2011). In particular, the patterns showed the reflections peaks on 2θ = 32.44°, 35.49°,38.72°, 48.7°, 53.40°, and 58.25° can be easily indexed to (110), (111)/(002), (111)/(200), (202), (020) and (202) crystal planes, respectively (JCPDS Card No. 45-937). However, no clear peaks corresponding to the anatase TiO$_2$ structure were observed. The peaks matching well with the anatase TiO$_2$, the relative peak around at 36.22° is indexed to the diffraction of the (111) plane of the CuO indicating that TiO$_2$ and CuO coexist in the CuO-TiO$_2$ heterojunction. This is understandable because the lattice constants of anatase TiO$_2$ are similar to those of CuO (Nguyen et al., 2013). Therefore, from diffraction pattern it can be concluded that crystalline CuO on TiO$_2$ has been formed.

Figure 4-2 The XRD diffraction patterns of the CuO-TiO$_2$

4.4 XPS analysis

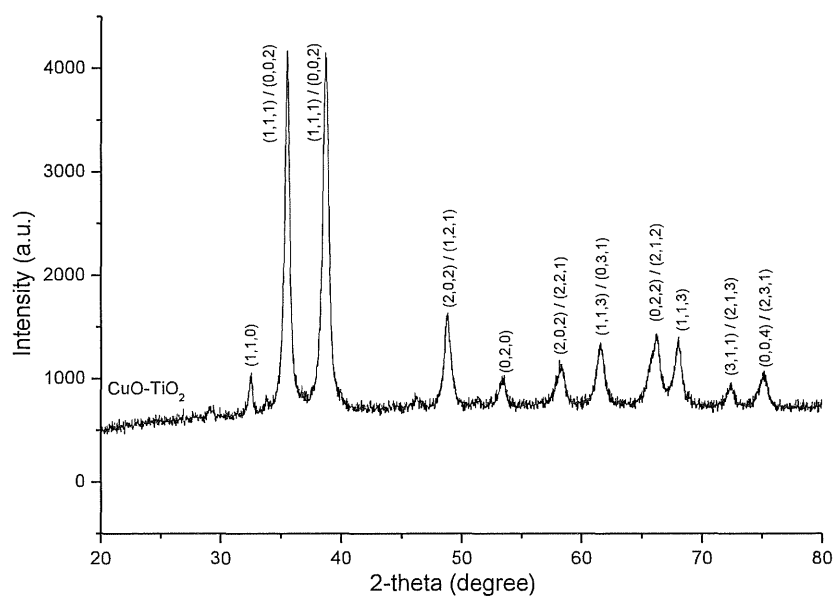The XPS spectra of Cu2p and O1s of the CuO-TiO$_2$ photocatalyst are presented in figure 4.3 and figure 4.4 and figure 4.5 respectively. Elements identified in narrow scan XPS survey spectra of the CuO-TiO$_2$ photocatalysts were the Cu2p, Ti2p, and O1s signals. It is clear that Cu2p3/2 and Cu2p1/2 spin orbital splitting photoelectrons are located at binding energies of 931.9 and 951.6 eV, respectively and is assigned to the compound of CuO and the peak located at 940.9 and 943.56 eV are attributed to the satellite peaks of CuO. XPS, therefore provides additional evidence for the formation of Cu^{2+} species in the junctions (Moniz et. al., 2015).

Following the figure 4.4, the spin orbit peaks of the Ti2p$_{3/2}$ and Ti2p$_{1/2}$ binding energy appeared around at 461.7 and 452.1 eV are assigned to Ti^{4+} ions (Park et al., 2016). As shown in Figure 4.5 the broad O 1s peak ranging from 523 to 543 eV in the XP spectrum is well-fitted by two components that have different energies. The binding energies have been identified as O^{2-} in CuO at 529.0 eV as indicated in peak (i) and oxygen adsorbed onto the surface of CuO photocatalyst at 530.6 eV in peak (ii). The O 1s peak can be deconvoluted using a peak procedure in which Gaussian peak shape was assumed to fit each component with a fixed binding energy as mentioned in (Hsieh et al., 2003). Therefore, the XPS result confirm that the samples contains CuO, which reflected no obvious change in chemical composition of the photocatalyst.
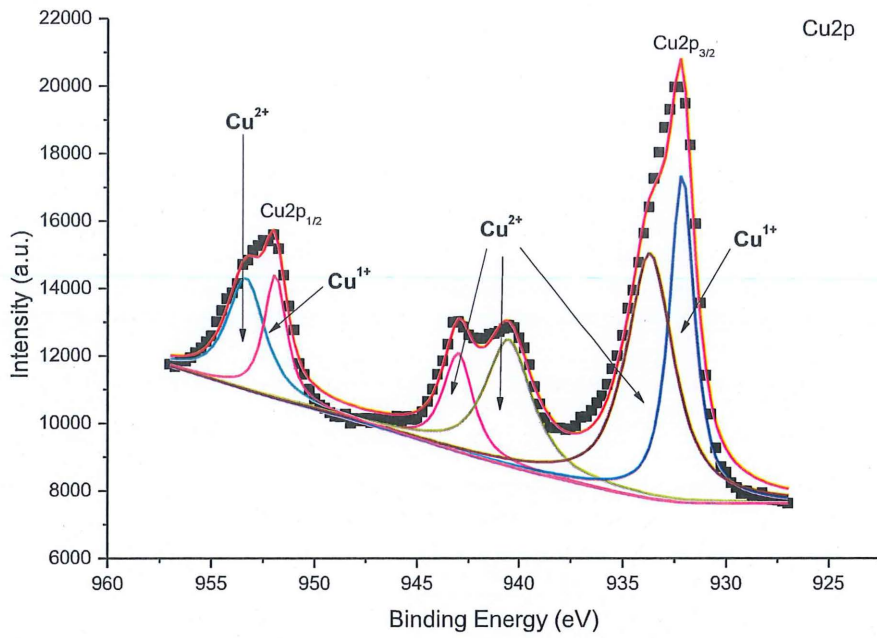
Figure 4-3 The XPS Spectra of the Cu2p
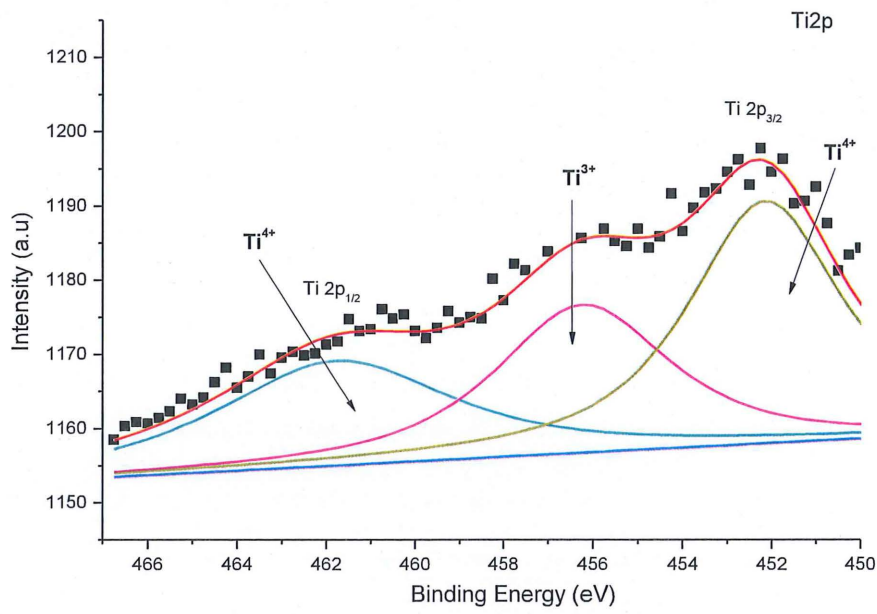
Figure 4-4 The XPS Spectra of the Ti2p
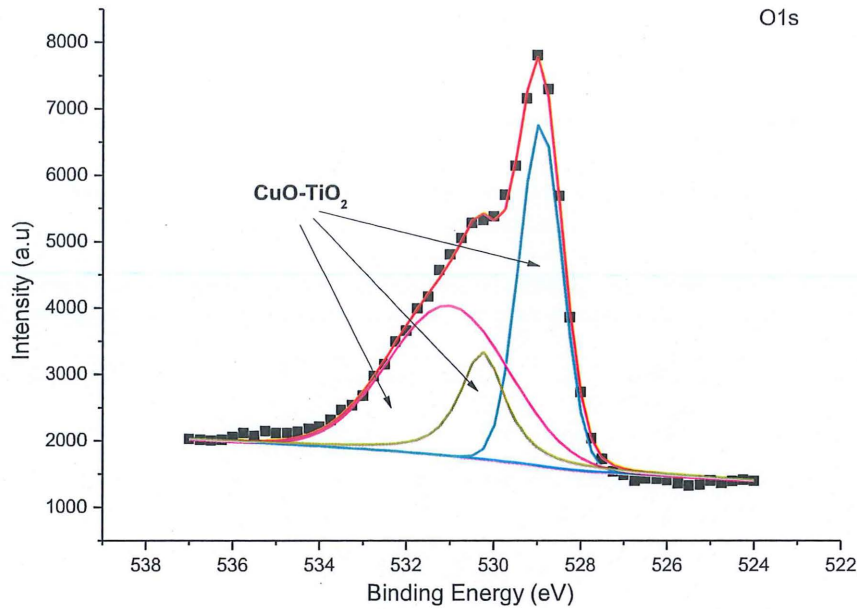
Figure 4-5 The XPS Spectra of the O1s

4.5 Photoluminescence Spectra Analysis

The purpose of PL emission spectra analysis was to reveal the efficiency of trapping, transfer and separation of charge carriers and to study the lifetime in semiconductor Figure 4.6 shows a PL spectra of the sample CuO-TiO$_2$ in the wavelength range of 200-700 nm at the same experimental conditions.

The PL spectrum of the as-prepared 1:1 molar ratio CuO-TiO$_2$ photocatalyst represented shows three main emission peaks appear at about 316, 373 and 677 nm, which are equivalent to 3.92, 3.32 and 1.83 eV respectively obtained from UV-Vis analysis. The strong peaks are about 316 nm arises from the band to band PL phenomenon approximately equal to the band gap energy of anatase and rutile (Yu, Hai, & Jaroniec, 2011). Besides that, at the PL peak of 373 and 677 nm are attributed to band edge free

excitations. However, in there is no PL spectra of commercial P25 TiO_2 comparison with $CuO-TiO_2$ photocatalyst in the present work.

It was expected from the literature that the intensity of TiO_2 band is higher compared to the $CuO-TiO_2$ catalyst. It represents that the rate of photogenerated electron-hole recombination of TiO_2 was higher than that of the CuO -TiO_2 catalyst (Jiao et al., 2014). The pattern of decline in PL intensity is due to the reduced number of recombination sites on the TiO_2 surface (Tseng et al., 2002). Fewer recombination sites on the surface lead to slower recombination of electrons and holes, thus a higher photocatalytic activity. Therefore, the copper-loaded titania effectively provides the electron traps and gives lower PL intensity resulting in higher methanol yield.
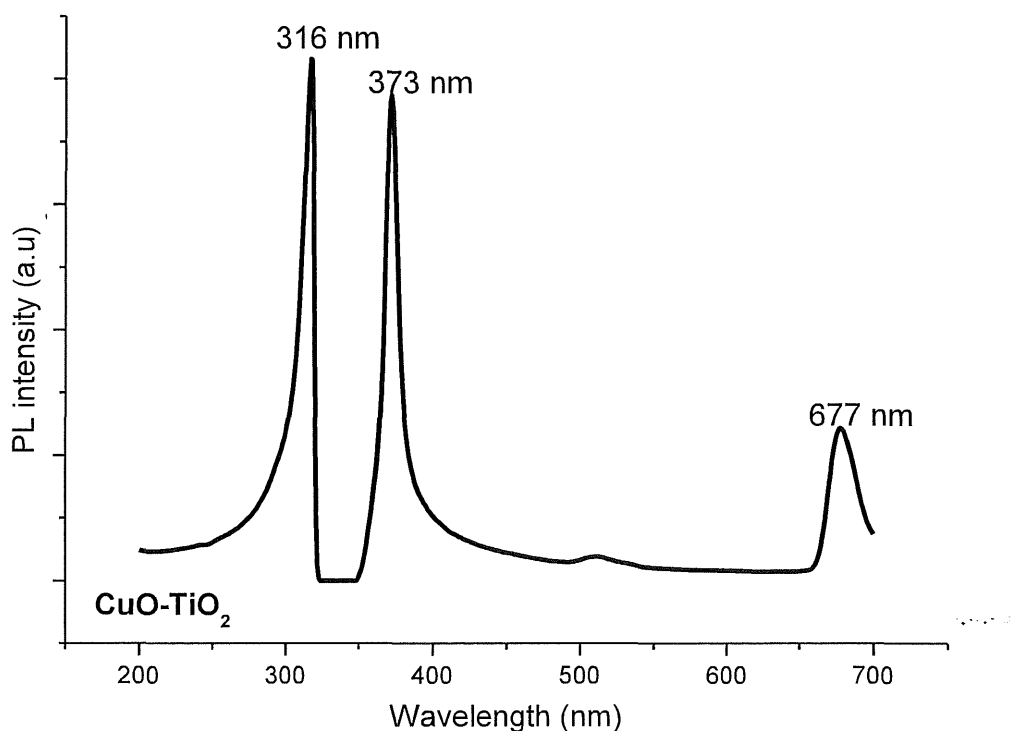
Figure 4-6 PL spectra of the sample $CuO-TiO_2$

4.6   Mott Schottky Analysis

As shown in Figure 4.7a, Mott-schottky analysis was carried out in a non-CO_2 bubbled 0.1 M $NaHCO_3$ solution (pH 6.8). E_{fb} is generally located near the VB, and it can be estimated from the intersection of a plot of $1/C^2$ against E as stated in equation 3.2 from the previous section. The x-axis intercept was 0.80 V versus NHE and the obtained flat band potential was estimated to be 0.83 V versus NHE. Figure 4.6b displays the band diagram for CuO-TiO_2 and the thermodynamic redox potential for the product of CO_2 reduction (V vs NHE). The   calculated VB and CB potential of CuO-TiO_2 were approximately -0.84 and -0.55 V versus a NHE, respectively. Given that a higher CB of CuO-TiO_2 than that of redox potential of CO_2, the excited electrons in the CB can easily transfer with assistance of an external bias potential leading to efficient photoelectrochemical reduction of CO_2 (Gu et al. 2013).

(b)

- $\cdot CO_2^-/CO_2$ (-1.90 V)
- CO/CO_2 (-0.53 V)
- $HCHO/CO_2$ (-0.48 V)
- CH_3OH/CO_2 (-0.40 V)
- CH_4/CO_2 (-0.24 V)
- O_2/H_2O (0.82 V)

Potential (V vs NHE)

Applied Potential

CB e^- e^- e^-

e

Light

VB

h^+
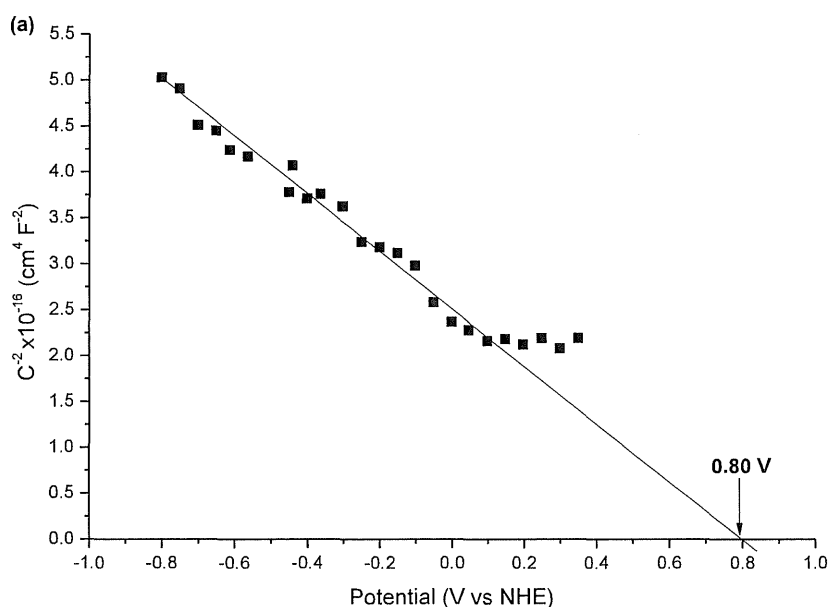
CuO-TiO$_2$

Figure 4-7**(a)** Mott-schottky plot of CuO-TiO$_2$ at 2000 Hz measured under dark condition; **(b)** Position of the conduction band and valence band of p-type CuO-TiO2 photocathode together with the redox potential of various reduction products at pH 7.

4.7   Photoelectrocatalytic (PEC) performance

4.7.1   Effect of light wavelength

The main factor that directly affects the initiation of a photoelectrochemical reaction is light, either it is UV or solar light. In photocatalytic reactions, UV lights are of common sources of illumination and usually provide 100-400 nm range of wavelength. Moreover, usage of light with a shor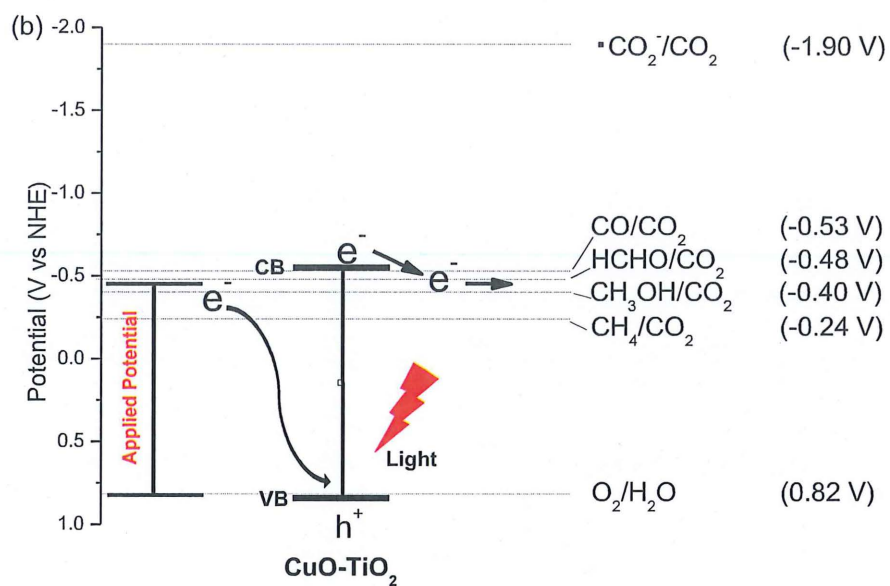ter wavelength for irradiation, is definitely more effective but not economical. It was known that, TiO_2 is a UV visible light catalyst. This studies the effect of wavelength on CuO supported on TiO_2 especially in visible light region. Therefore, the selection of the optimum light for a specific semiconducting material in a photoelectrochemical reaction is of vital interest.

Light source of XD-300 High Brightness Cold Light Source, Beijing Perfect light Co., Ltd., China was used during experiment. Apart from that, different light filters with the wavelength of 470, 650 and 750 nm have been exploited in the current work to explore and optimize the effect of light on the photoelectrocatalytic activity. Comparison of the effect of light wavelength is shown in Fig. 4-8. The results indicate that the The observed onset potential at 470 nm wavelength was at -0.20 V versus NHE whereas no apparent peaks are obtained at higher light conditions (650 and 730 nm). Besides, the shoulder observed during light off condition was shifted toward lower potential region and no peak was detected under light illumination at 650 and 730 nm wavelengths. Whereas, a characteristic peak was detected at -0.20V versus NHE when light illuminated at 470 nm indicating lower wavelength number is more favourable towards CO_2 reduction reaction.
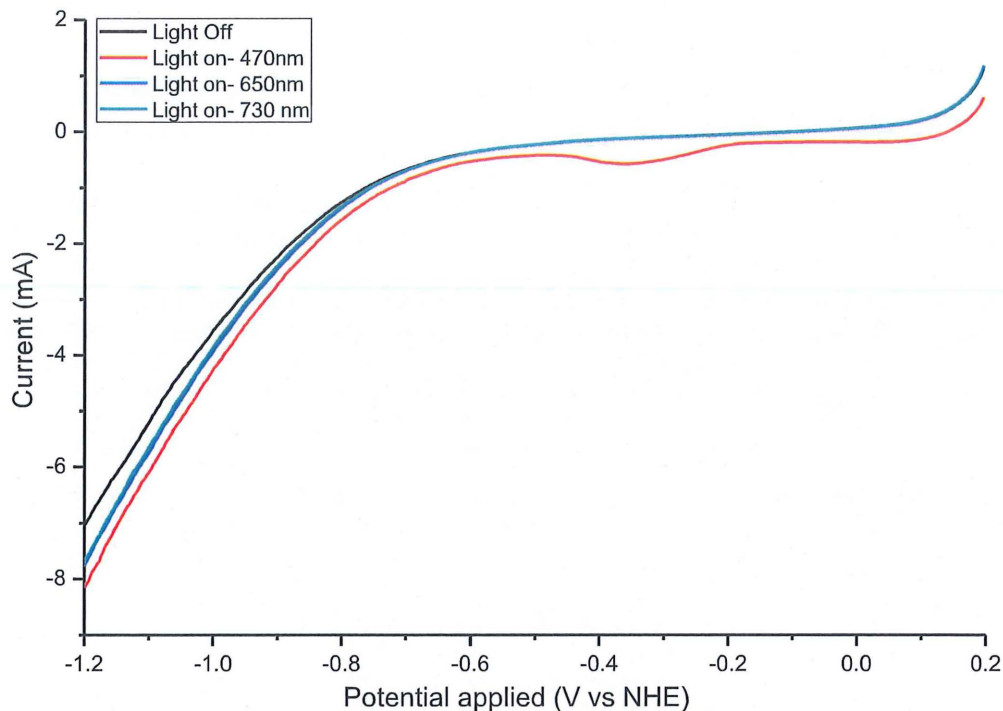
Figure 4-8 Effect of different light wavelength of CuO-TiO$_2$ electrode in CO$_2$-saturated 0.1 M NaHCO$_3$ solution

4.7.2 Linear Sweep Voltammetry

The linear scan voltammograms for CuO-TiO$_2$ in 0.1M NaHCO$_3$ for 4.9(a) N$_2$-saturated and whereas 4.10(a) commercial TiO$_2$ in 0.1M NaHCO$_3$ and 4.10(b) for CuO-TiO$_2$ in 0.1M NaHCO$_3$ CO$_2$-saturated under dark and visible light illumination at 10 mV/s. It can be seen that, the shape of the voltammogram in inert condition presents similar patterns during light on and light off (Lee et al. 2014). The cathodic current was increased as the applied potential increased for light on compared to light off condition. These phenomenon might be due to water/proton reduction (Shen et al. 2015).

While in CO$_2$-saturated condition it was observed that with or without light irradiation, commercial TiO$_2$ nanoparticle photoelectrode exhibited a poor photocurrent response, figure 4.8(a) might be due to the large band gap that only can be utilize in UV light region (Ansari et. al., 2016). In contrast, cathodic current profile of CuO-TiO$_2$ was

improved with the increase copper loading. The as prepared $CuO-TiO_2$ onset potential value from -0.20V vs NHE with current peak potential appearing at -0.36V vs NHE. A slight shift of onset potential to less negative region, indicating the reaction could occur with less applied potential which suggesting an excellent photocatalyst $CuO-TiO_2$. Table 4-1 summarizes the onset potential and peak potential of the photocatalyst in CO_2-saturated obtained from LSV experiment.
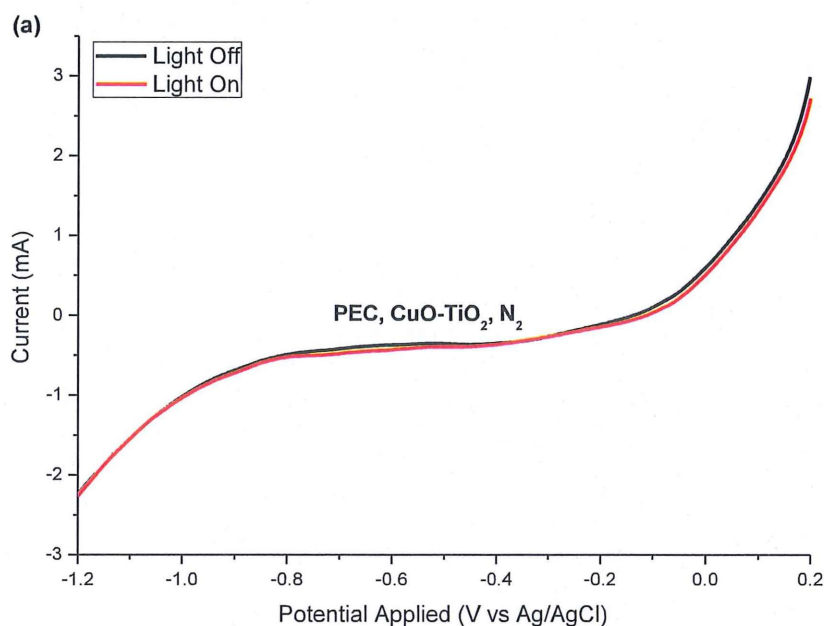
Figure 4-9 LSV of $CuO-TiO_2$ electrode in N_2-saturated 0.1 M $NaHCO_3$ solution under light on/off (scan rate 10 mV/s; light wavelength = 470 nm)
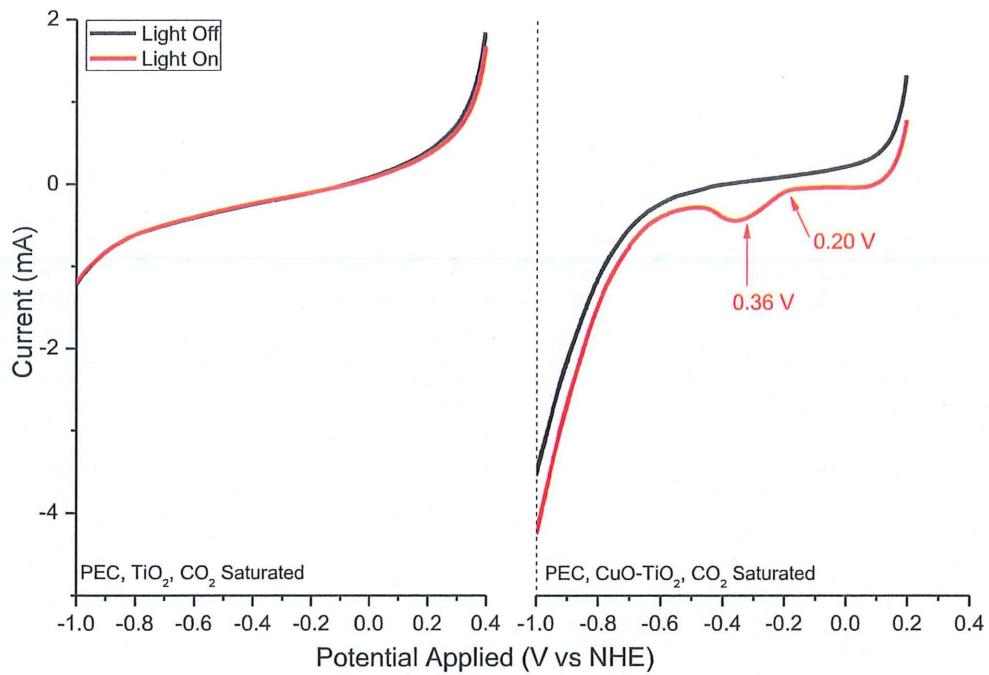
Figure 4-10 (a) LSV of commercial TiO_2 electrode (calcined 500°C, 5 hr) and (b) LSV of CuO-TiO_2 electrode in CO_2-saturated 0.1 M $NaHCO_3$ solution under light on/off (scan rate 10 mV/s; light wavelength = 470 nm)

Table 4-1: Onset potential and peak potential of the photocatalyst in CO_2-saturated

Catalyst	Onset Potential (V vs NHE)	Peak Potential (V vs NHE)	Bandgap[a] (eV)
Commercial TiO_2	-	-	3.1
1:1 CuO-TiO_2	-0.20	-0.36	1.12

[a] Estimated from UV-Vis spectra

4.7.3 Photoelectrocatalytic activity towards CO₂ reduction

The photoelectrochemical reduction of CO_2 and the yields of methanol, CH_3OH on CuO-TiO_2 photocatalyst was investigated under a period of 4 hours under visible light irradiation as shown in figure 4.11. The main product of the liquid phase were expected to be methanol followed $2e^-$, $4e^-$ and $8e^-$ pathway as shown in Eqs. (3-6):

$$CO_2 + 2H^+ + 2e^- \rightarrow CO + H_2O \tag{3}$$

$$CO_2 + 2H^+ + 2e^- \rightarrow HCOOH \tag{4}$$

$$CO_2 + 6H^+ + 6e^- \rightarrow CH_3OH + H_2O \tag{5}$$

$$CO_2 + 8H^+ + 8e^- \rightarrow CH_4 + 2H_2O \tag{6}$$
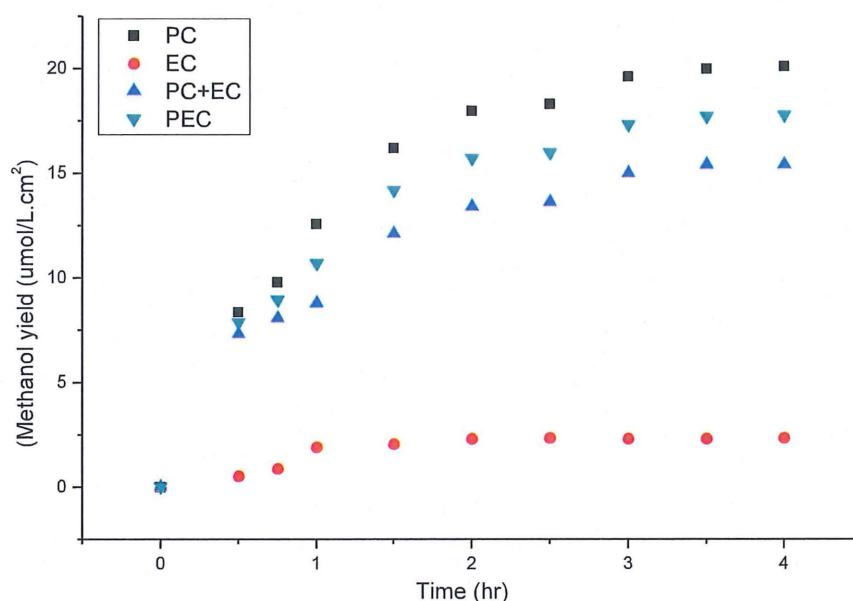
Figure 4-11: Methanol yields under photoelectrocatalytic (PEC), electrocatalytic (EC) and photcatalytic (PC) condition with 4 hours visible light irradiation on CuO-TiO_2 electrode.

Figure 4.11 shows the product yield The PEC, EC and PC reduction of CO_2 were conducted in 250 ml of CO_2-saturated 0.1 M $NaHCO_3$ solution at -0.55 V under visible-light irradiation. In this work, methanol was found as the main product in the liquid phase as tested in GC-FID. It was found out that during blank experiment (in 0.1 mol $NaHCO_3$

solution without CO_2 purging), no other C1 products obtained, proving that carbon in CH_3OH originated from the injected CO_2. With CuO-TiO_2 electrode, the methanol yield increased as irradiation time progressed. At 4 h reaction time, amount of methanol yield for PC, EC and PEC was monitored to be 2.35, 15.40 and 20.1 $\mu mol.L^{-1}.cm^{-2}$ respectively.

The PEC activities obtained on the CuO-TiO_2 revealed the importance of CuO cocatalyst help to improve the photocatalytic performance of TiO_2 suggesting the CB of CuO-TiO_2 obtained was -0.55 V versus NHE which was more negative than the reduction potential of CO_2/CH_3OH (-0.40 V vs. NHE). Moreover, the resulting methanol yield in PEC system are better compared to the summation of EC and PC (17.75 $\mu mol.L^{-1}.cm^{-2}$) processes. Thus, the EC and PC reductions of CO_2 on CuO-TiO_2 confirming the synergistic effect in term of product yield.

The production rate and compositions of the hydrocarbon is highly dependent on the PEC reactor, applied bias potential and catalyst materials. It is necessary to further investigate the detailed elementary reactions and distributed products in multiple pathways. Moreover, the product identification by chromatography method could be useful to confirm the mechanism of the reaction. Two reactions occurred on the electrode surface under irradiation:

(i) water was oxidized by the photogenerated holes to protons and oxygen because of the valence band at 1.09 eV, which was higher than the oxidation potential of H_2O/O_2 (0.82 V vs. NHE). Therefore, the as-prepared material could supply enough protons for CO_2 reduction by the valence-band oxidation.

(ii) CO_2 could be reduced to CH_3OH (P. Li et al., 2014). On one hand, the suitable conduction band of the as-prepared CuO-TiO_2 was -0.55 eV, which was more negative than the reduction potential of CO_2/CH_3OH (-0.4 V vs. NHE), which indicated that the catalyst possessed enough PC reductive ability to reduce CO_2 to CH_3OH .

Besides, the external bias potential could not only enhance the separation of electrons and holes to improve the PC reduction of CO_2 but also supplied sufficient electrons to sustain the EC reduction of CO_2. Thus, the high efficiency of the PEC synergistic reduction of CO_2 on the CuO-TiO_2 could be reasonably explained.

4.8   Reaction Mechanism

All energy was provided by the solar cell. The mechanism for photoelectrochemical reduction of CO_2 in a $NAHCO_3$ aqueous solution with a $CuO\text{-}TiO_2$ electrode was investigated. The photocatalytic reduction mechanism of CO_2 is a complex phenomenon, where two aspects regarding the rate-limiting step should be taken into consideration. As mentioned before, CO_2 is a thermodynamically stable and chemically inert compound and it is difficult to oxidize or reduce it to various intermediate chemicals under normal operating conditions.

Possible mechanism was proposed for the PEC reduction of CO_2 to methanol in figure 4.12. Within the $CuO\text{-}TiO_2$ photocatalyst, the electrons (e^-) and holes (h^+) recombination process was inhibited due to the external bias potential contribute electron to VB to the photoreduction of adsorbed CO_2. Upon visible light driven, photoelectrons generated from $CuO\text{-}TiO_2$ at VB jumps to CB, and promote the flows to CO_2 due to the band bending between the interface of the photocatalyst. The possible reaction that might happen on the electrode surface under irradiation:

(i) Water was oxidized in anode chamber and produced oxygen, protons and electrons. The generated protons were transfer through the proton exchange membrane and diffuse to the cathode. Thus $CuO\text{-}TiO_2$ could supply enough protons for CO_2 reduction.

(ii) The CB of $CuO\text{-}TiO_2$ was -0.53 V versus NHE which was more negative than the reduction potential of CO_2/CH_3OH (-0.40 V vs. NHE), indicating that the catalyst possessed enough PC reductive ability to reduce CO_2 to CH_3OH.

On the other hand, the external potential could not only enhance the separation of electrons and holes to improve the PC reduction of CO_2 but also supplied sufficient electrons to sustain the EC reduction of CO_2. However, the efficiency of the reaction could be low, due to the electron-hole (e-/h+) recombination process. Therefore, at a minimum potentials of -0.36 V vs NHE, can assist CO_2 reduction and is important for selective product production. The PEC result was compared with only electrocatalysis (EC) and photocatalysis (PC) possesses two advantages (Huang, Cao, Liu, & Zhao, 2013):

(i) the application of certain electrode potential not only assists specific electrode reaction but also facilitates the separation of photoinduced carrier, enhancing PC process.

(ii) Solar light irradiation lowers the electrochemical barrier and promotes the electrode kinetics for a specific reaction, favouring the EC process. Thus capable to reduce CO_2 to CH_3OH.
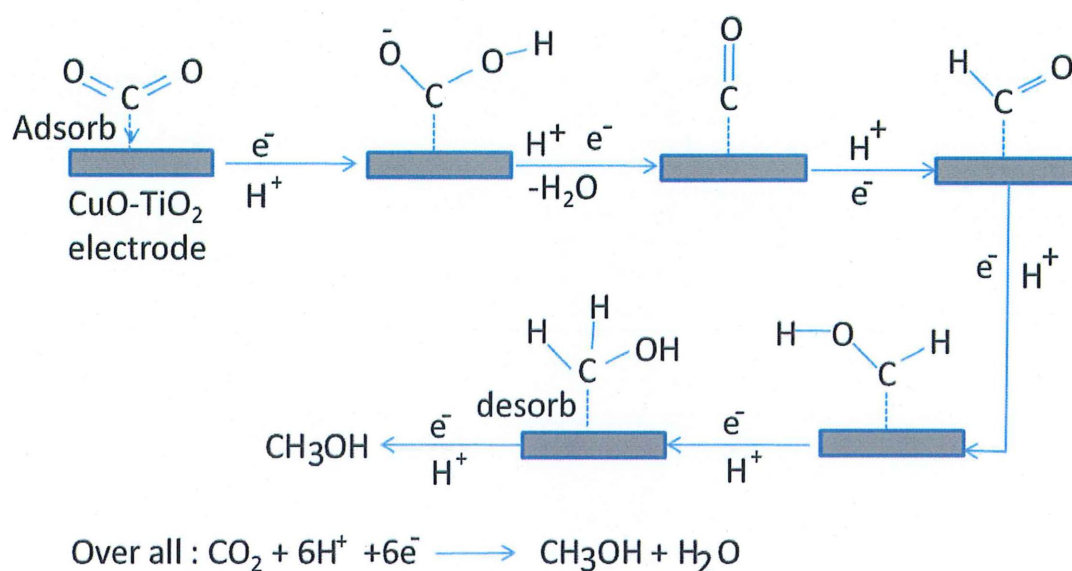

Over all : $CO_2 + 6H^+ + 6e^- \longrightarrow CH_3OH + H_2O$

Figure 4-12 Scheme of CO_2 photoreduction mechanism on CuO-TiO$_2$ catalyst

To activate the inert CO_2 molecule for reduction, the best way is to adsorb it on surface of CuO-TiO$_2$ catalyst electrode. If a high-dielectric-constant solvent is used such as water, the CO_2 - anion radicals can be greatly stabilized by the solvent, resulting in weak interactions with the photocatalyst surface. After the adsorption, upon visible light irradiation, electrons and holes are produced and reaction initiates. Electron reached to the adsorbed CO_2 and reduced it to an anion radical $\cdot CO_2^-$ whereas, H_2O oxidation proceeds through the holes, which make H^+, $\cdot OH$ or O_2, which is being desorbed or further, participate in the reaction. The H^+ further takes electron and form $\cdot H$, which reacts with the $\cdot CO2^-$ to make CO and OH^-.

CHAPTER 5

CONCLUSION AND RECOMMENDATION

5.1   Conclusions

The aim of this study was to synthesize and characterize CuO-TiO_2 as a light responsive catalyst that to be applied in CO_2 photoelectrochemical reduction into methanol under visible light irradiation. The CuO-TiO_2 photocatalyst was prepared at different molar ratio via sol-gel method. The photocathode catalyst for photoelectrochemical (PEC) reduction of CO_2. XRD, XPS, PL, UV-Vis and mott-schottky (MS) experiments were employed to characterize the photocatalyst. Linear sweep voltammetry (LSV) was employed to evaluate the effect of visible light ($\lambda > 400$ nm) on activity for CO_2 reduction.

The structure of a catalyst plays crucial roles in CO_2 reduction through affecting either the separation of photogenerated electron-hole pairs or the reactivity of catalyst surfaces or both. For instance, the crystalline phase of CuO-TiO_2 affected its photocatalytic activity for CO_2 reduction not only because of the different crystalline and electronic structures but also due to the different concentration of surface defective sites (Ti^{3+} sites and oxygen vacancies), which may be responsible for CO_2 reduction.

Next from the mott schottky analysis, the calculated VB and CB potential of CuO-TiO_2 were approximately -0.83 and -0.55 V versus a NHE, respectively. Given that a higher CB of CuO-TiO_2 than that of redox potential of CO_2, the excited electrons in the CB can easily transfer with assistance of an external bias potential leading to efficient photoelectrochemical reduction of CO_2

The PEC reaction contributed to higher methanol yield than PC and EC reaction giving a maximum yield of 20.1 $\mu mol.L^{-1}.cm^{-2}$ over CuO-TiO$_2$. An electron flow scheme was proposed to demonstrate the possible occurred CO$_2$ reduction reaction. The possible reduced product were carbon monoxide, formic acid, methanol and methane, as their redox potential was lower compared to CB value. With the potential being more negative, the reduction of CO$_2$ became more significant with the PEC effect directly related with the applied potential. This suggest that the separation of photo- induced carrier and hole was also more effective under more negative potential, and it enabled more photoelectrons arrive at the surface active sites.

5.2   Recommendations

For future improvement, in order to gain ideal crystal growth which give good electronic structures and surface transfer of photoinduced change carriers on the photoreduction process, the design of photocatalyst configuration and its distribution of dopants CuO in TiO$_2$ particles should be further investigate. It is important to control the surface heteroatomic structure of TiO$_2$ to guarantee the photoinduced electrons and holes are powerful enough, under solar irradiation, to promote surface charge-carrier transfer for successive photoreduction. The recommendation to enhance the properties of the prepared catalysts are based on the preparation of catalyst and its characterization.

5.2.1   Preparation of catalyst

In term of catalyst preparation, there should be various parameters should be considered as it will affect the properties of the prepared catalyst. The consideration on the weight (wt%) of the CuO to TiO$_2$, calcination temperature, precursor used should be further investigate through sol-gel method.

5.2.2   Characterization of catalyst

In term of characterization, more analysis should be fully utilized to further study on the catalyst characteristic. For instance, TEM and SEM analysis to clearly display the morphology of the catalyst. Besides that, EDX results can be used to fully examine the catalyst properties.

REFERENCES

Albo, J., Alvarez-Guerra, M., Castaño, P., & Irabien, A. (2015). Towards the electrochemical conversion of carbon dioxide into methanol. *Green Chemistry*, *17*(4), 2304-2324.

Ampelli, C., Centi, G., Passalacqua, R., & Perathoner, S. (2016). Electrolyte-less design of PEC cells for solar fuels: Prospects and open issues in the development of cells and related catalytic electrodes. *Catalysis Today*, *259*, 246–258. https://doi.org/10.1016/j.cattod.2015.07.020

Ansari, S. A., & Cho, M. H. (2016). Highly Visible Light Responsive , Narrow Band gap TiO 2 Nanoparticles Modified by Elemental Red Phosphorus for Photocatalysis and Photoelectrochemical Applications. *Nature Publishing Group*, (April), 1–10. https://doi.org/10.1038/srep25405

Ansari, S. A., Khan, M. M., Ansari, M. O., & Cho, M. H. (2015). Gold nanoparticles-sensitized wide and narrow band gap TiO 2 for visible light applications: a comparative study. *New J. Chem.*, *39*(6), 4708–4715. https://doi.org/10.1039/C5NJ00556F

Bachu, S., Bonijoly, D., Bradshaw, J., Burruss, R., Holloway, S., Christensen, N. P., & Mathiassen, O. M. (2007). CO2 storage capacity estimation: Methodology and gaps. *International Journal of Greenhouse Gas Control*, *1*(4), 430–443. https://doi.org/10.1016/S1750-5836(07)00086-2

Barreca, D., Carraro, G., Comini, E., Gasparotto, A., Maccato, C., Sada, C., … Tondello, E. (2011). Novel Synthesis and Gas Sensing Performances of CuO À TiO 2 Nanocomposites Functionalized with Au Nanoparticles, 10510–10517.

Benson, E. E., Kubiak, C. P., Sathrum, A. J., & Smieja, J. M. (2009). 2009 Renewable Energy issue energy research to liquid fuels w, (1). https://doi.org/10.1039/b804323j

Brito, J. F. De, Alves, A., & Cavalheiro, A. J. (2014). Evaluation of the Parameters Affecting the Photoelectrocatalytic Reduction of CO 2 to CH 3 OH at Cu / Cu 2 O Electrode, *9*(Cv), 5961–5973. https://doi.org/10.1016/j.fuel.2015.09.082

Carp, O., Huisman, C. L., & Reller, A. (2004). Photoinduced reactivity of titanium dioxide. *Progress in Solid State Chemistry*, *32*(1–2), 33–177. https://doi.org/10.1016/j.progsolidstchem.2004.08.001

Djurišić, A. B., Leung, Y. H., & Ching Ng, A. M. (2014). Strategies for improving the efficiency of semiconductor metal oxide photocatalysis. *Materials Horizons*, *1*(4), 400. https://doi.org/10.1039/c4mh00031e

Ganesh, I. (2014). Conversion of carbon dioxide into methanol – a potential liquid fuel :

Fundamental challenges and opportunities (a review), *31*, 221–257.

Guo, L. J., Wang, Y. J., & He, T. (2016). Photocatalytic Reduction of CO2 over Heterostructure Semiconductors into Value-Added Chemicals. *Chemical Record*, 1918–1933. https://doi.org/10.1002/tcr.201600008

Hsieh, C., Chen, J., Lin, H., Shih, H., Hsieh, C., & Chen, J. (2003). Field emission from various CuO nanostructures Field emission from various CuO nanostructures, *3383*, 10–13. https://doi.org/10.1063/1.1619229

Huang, X., Cao, T., Liu, M., & Zhao, G. (2013). Synergistic Photoelectrochemical Synthesis of Formate from CO 2 on { 121⁻} Hierarchical Co 3 O 4.

Jiao, J., Wei, Y., Zhao, Z., Liu, J., Li, J., Duan, A., & Jiang, G. (2014). Photocatalysts of 3D Ordered Macroporous TiO 2 - Supported CeO 2 Nanolayers : Design , Preparation , and Their Catalytic Performances for the Reduction of CO 2 with H 2 O under Simulated Solar Irradiation.

K. C. Mathai, S. Vidya, Annamma John, Sam Solomon, and J. K. Thomas, "Structural, Optical, and Compactness Characteristics of Nanocrystalline CaNb$_2$O$_6$ Synthesized through an Autoigniting Combustion Method," Advances in Condensed Matter Physics, vol. 2014, Article ID 735878, 6 pages, 2014. doi:10.1155/2014/735878

Karamian, E., & Sharifnia, S. (2016). On the general mechanism of photocatalytic reduction of CO 2, *16*, 194–203.

Kočí, K., Matějová, L., Reli, M., Čapek, L., Matějka, V., Lacný, Z., ... Obalová, L. (2014). Sol–gel derived Pd supported TiO2-ZrO2 and TiO2 photocatalysts; their examination in photocatalytic reduction of carbon dioxide. *Catalysis Today*, *230*, 20–26. https://doi.org/10.1016/j.cattod.2013.10.002

Li, H., Li, C., Han, L., Li, C., & Zhang, S. (2016). Environmental Effects Photocatalytic reduction of CO 2 with H 2 O on CuO / TiO 2 catalysts, *7036*(February). https://doi.org/10.1080/15567036.2011.598910

Li, P., Jing, H., Xu, J., Wu, C., Peng, H., Lu, J., & Lu, F. (2014). High-e ffi ciency synergistic conversion of CO 2 to methanol using Fe 2 O 3 nanotubes modi fi ed with double-layer Cu 2 O spheres †, 11380–11386. https://doi.org/10.1039/C4NR02902J

Marszewski, M., Cao, S., Yu, J., & Jaroniec, M. (2015). Semiconductor-based photocatalytic CO 2 conversion. *Mater. Horiz.*, *2*(3), 261–278. https://doi.org/10.1039/C4MH00176A

Moniz, S. J. A., & Tang, J. (2015). Charge Transfer and Photocatalytic Activity in CuO / TiO 2 Nanoparticle Heterojunctions Synthesised through a Rapid , One-Pot , Microwave Solvothermal Route, 1659–1667. https://doi.org/10.1002/cctc.201500315

Nasution, H. W., Purnama, E., Riyani, K., & Gunlazuardi, J. (2009). Effect of Copper Species in a Photocatalytic Synthesis of Methanol from Carbon Dioxide over Copper-doped Titania Catalysts, *6*(1), 112–122.

Nikokavoura, A., & Trapalis, C. (2016). Article in press, 1–26. https://doi.org/10.1016/j.apsusc.2016.06.172

Ola, O., & Maroto-valer, M. M. (2015). Journal of Photochemistry and Photobiology C : Photochemistry Reviews Review of material design and reactor engineering on TiO 2 photocatalysis for CO 2 reduction. *"Journal of Photochemistry & Photobiology, C: Photochemistry Reviews,"* *24,* 16–42. https://doi.org/10.1016/j.jphotochemrev.2015.06.001

Park, S., Razzaq, A., Park, Y. H., Sorcar, S., Park, Y., & Grimes, C. A. (2016). Hybrid Cu x O − TiO 2 Heterostructured Composites for Photocatalytic CO 2 Reduction into Methane Using Solar Irradiation : Sunlight into Fuel. https://doi.org/10.1021/acsomega.6b00164

Portenkirchner, E., Oppelt, K., Ulbricht, C., Egbe, D. A. M., Neugebauer, H., Knör, G., & Serdar, N. (2012). Electrocatalytic and photocatalytic reduction of carbon dioxide to carbon monoxide using the alkynyl-substituted rhenium (I) complex (5 , 5 0 - bisphenylethynyl-2 , 2 0 -bipyridyl) Re (CO) 3 Cl, *716,* 19–25. https://doi.org/10.1016/j.jorganchem.2012.05.021

Qin, S., Xin, F., Liu, Y., Yin, X., & Ma, W. (2011). Photocatalytic reduction of CO2 in methanol to methyl formate over CuO-TiO2 composite catalysts. *Journal of Colloid and Interface Science, 356*(1), 257–261. https://doi.org/10.1016/j.jcis.2010.12.034

Ramli, R., Khan, M. R., Yunus, R. M., Ong, H. R., Halim, R. M., Aziz, A. A., Institusi, P. (2014). In-Situ Impregnation of Copper Nanoparticles on Palm Empty Fruit Bunch Powder. *Advances in Nanoparticles,* *3*(August), 65–71. https://doi.org/dx.doi.org/10.4236/anp.2014.33009

Sarkar, A., Gracia-Espino, E., Wågberg, T., Shchukarev, A., Mohl, M., Rautio, A. R., … Mikkola, J. P. (2016). Photocatalytic reduction of CO2 with H2O over modified TiO2 nanofibers: Understanding the reduction pathway. *Nano Research, 9*(7), 1956–1968. https://doi.org/10.1007/s12274-016-1087-9

Sudhagar, P., Roy, N., Vedarajan, R., & Devadoss, A. (2016). *Hydrogen and CO 2 Reduction Reactions : Mechanisms and Catalysts.* https://doi.org/10.1007/978-3-319-29641-8

Thi Hiep Nguyen, Thu Loan Nguyen, T. D. T. U. and Q. L. N. (2013). Synthesis and characterization of nano-CuO and CuO / TiO 2 photocatalysts. *Advances in Natural Science: Nanoscience and Nanotechnology,* 25002. https://doi.org/10.1088/2043-6262/4/2/025002

Tseng, I., Chang, W., & Wu, J. C. S. (2002). Photoreduction of CO 2 using sol − gel derived titania and titania-supported copper catalysts. *Applied Catalysis B: Environmental, 37,* 37–48.

Wang, K., Yu, J., Liu, L., Hou, L., & Jin, F. (2016). Hierarchical P-doped TiO2 nanotubes array@Ti plate: Towards advanced CO2 photocatalytic reduction catalysts. *Ceramics*

International, 42(14), 16405–16411. https://doi.org/10.1016/j.ceramint.2016.07.149

Wang, W. N., Soulis, J., Jeffrey Yang, Y., & Biswas, P. (2014). Comparison of CO2 photoreduction systems: A review. *Aerosol and Air Quality Research, 14*(2), 533–549. https://doi.org/10.4209/aaqr.203.09.0283

Xie, S., Zhang, Q., Liu, G., & Wang, Y. (2015). reduction of CO 2 using heterogeneous catalysts with controlled nanostructures. *Chemical Communications, 52,* 35–59. https://doi.org/10.1039/C5CC07613G

Yamashita, H., Harada, M., Misaka, J., Takeuchi, M., Ikeue, K., & Anpo, M. (2002). Degradation of propanol diluted in water under visible light irradiation using metal ion-implanted titanium dioxide photocatalysts. *Journal of Photochemistry and Photobiology A: Chemistry, 148*(1–3), 257–261. https://doi.org/10.1016/S1010-6030(02)00051-5

Yoon, T. P., Ischay, M. a, & Du, J. (2010). Visible light photocatalysis as a greener approach to photochemical synthesis. *Nature Chemistry, 2*(7), 527–532. https://doi.org/10.1038/nchem.687

Yu, J., Hai, Y., & Jaroniec, M. (2011). Journal of Colloid and Interface Science Photocatalytic hydrogen production over CuO-modified titania. *Journal of Colloid And Interface Science, 357*(1), 223–228. https://doi.org/10.1016/j.jcis.2011.01.101

APPENDICES

APPENDIX A: ANALYSIS SUPPORTING INFORMATION

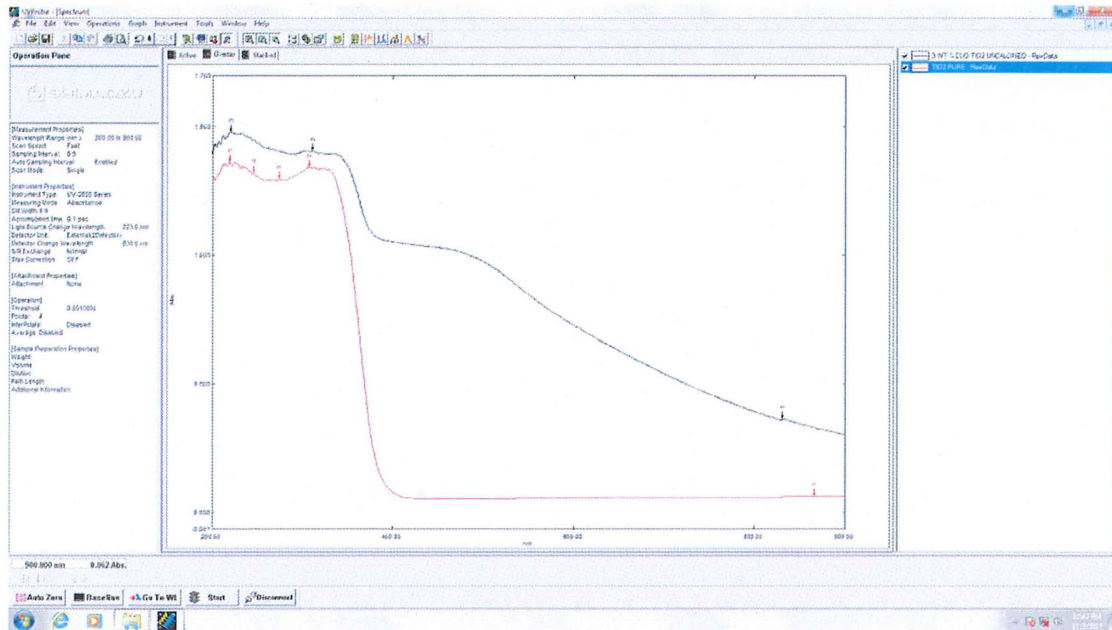### APPENDIX A.1: UV-vis spectroscopy supporting information

Figure S1: UV-vis spectroscopy supporting information

APPENDIX A.2: XRD analysis supporting information

Table A.1: Measurement conditions and qualitative analysis results

Measurement conditions

X-Ray	30 kV , 15 mA	Scan speed / Duration time	1.0000 sec
Goniometer		Step width	0.0200 deg.
Attachment	-	Scan axis	2Theta/Theta
Filter		Scan range	3.0000 -
CBO selection	-	Incident slit	1.25 deg.
Diffrected	Fixed	Length limiting	-
Detector	MiniFlex2	Receiving slit	1.25 deg.
Scan mode	STEP	Receiving slit	0.3mm

Qualitative analysis results

Phase name	Formula	Figure of merit	Phase reg. detail	DB card number
Tenorite	Cu O	0.282	User	9016057
Baddeleyite	O2 Ti	3.347	User	9015355

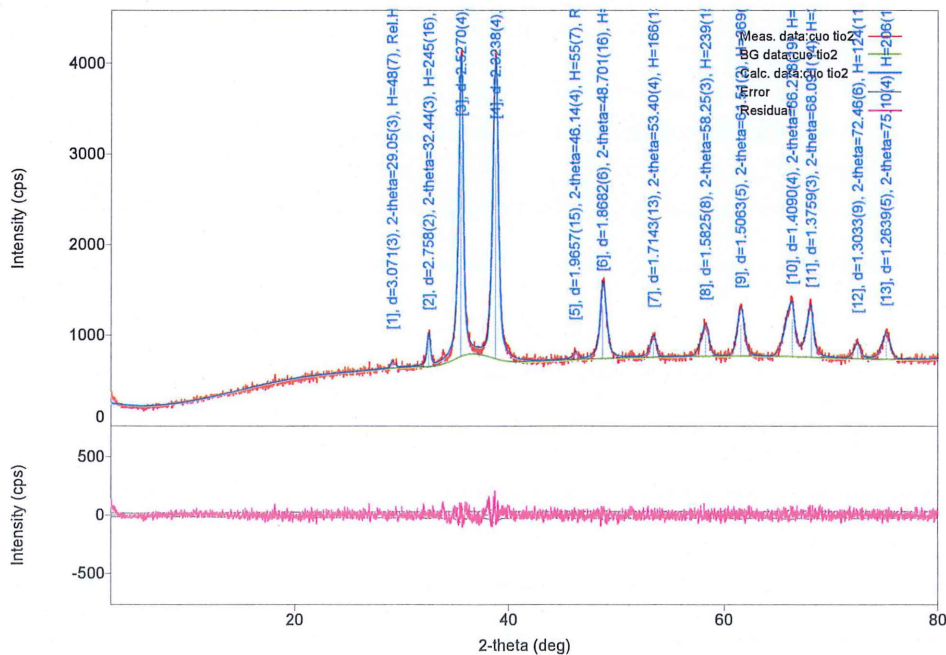| Phase name	Formula	Space group	Phase reg. detail	DB card number
Tenorite	Cu O	9	: User	9016057
Baddeleyite	O2 Ti	14	: User	9015355

Figure S2: XRD analysis supporting information

APPENDIX A.3: XPS analysis supporting information

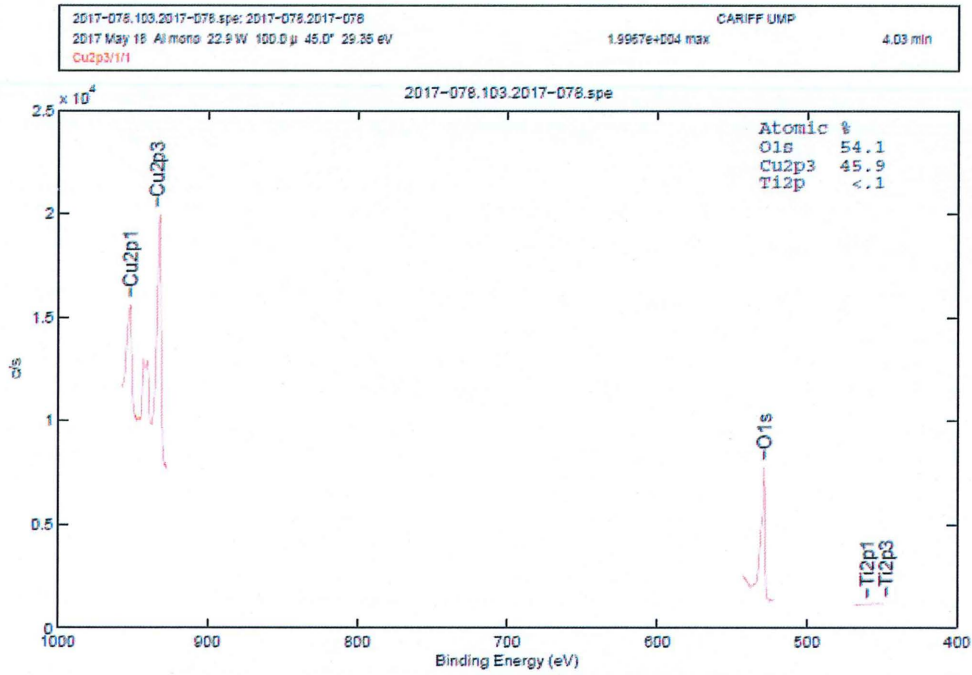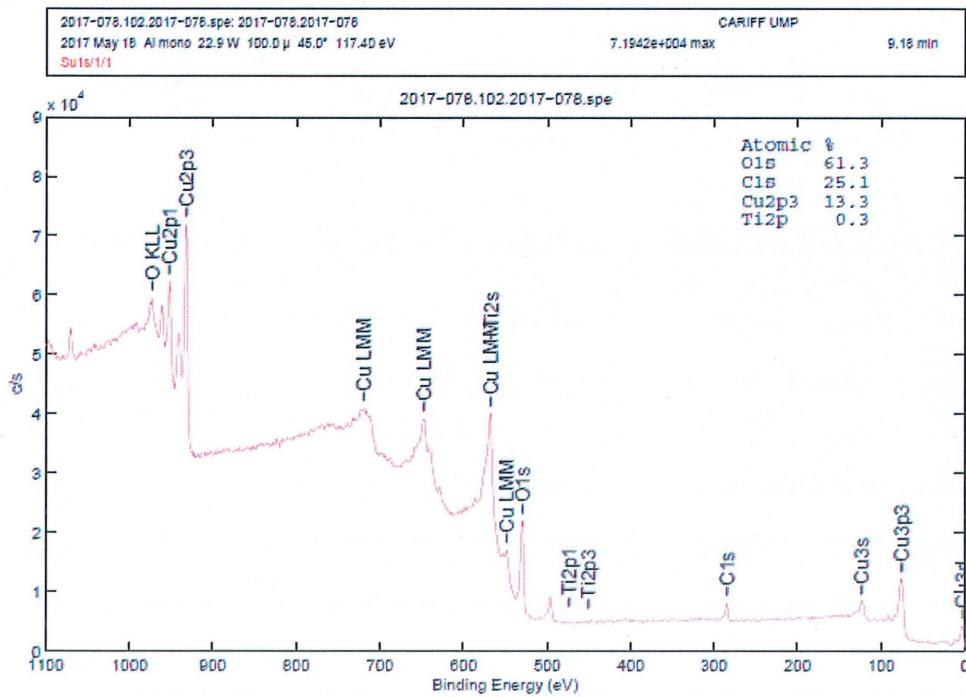**Figure S3:** Narrow scan result supporting information

Figure S4: Survey scan result supporting information